A Spectrally Efficient Signal Space Diversity-Based Two-Way Relaying System

Hamza Umit Sokun, *Student Member, IEEE*, Mehmet Cagri Ilter, *Student Member, IEEE*, Salama Ikki, *Member, IEEE*, and Halim Yanikomeroglu, *Fellow, IEEE*

***Abstract*—This work proposes a new transmission scheme for multirelay two-way relaying systems, where two end- sources communicate with each other via a set of relays. In the proposed scheme, we consider signal space diversity and time division broadcast protocol jointly to increase spectral efficiency without sacrificing the system reliability. The idea behind this consideration is that original data symbols are rotated before transmission, and then the inphase and quadrature components of these rotated symbols are transmitted through the cooperation of the end-sources and the relays. By doing so, the end-sources exchange four symbols over three time slots instead of two, i.e., doubling the number of transmitted symbols. In addition, relay selection is incorporated into this scheme to achieve a further increase in spectral efficiency. For relay selection, two different strategies are discussed: reactive and proactive relay selections. These strategies differ depending on whether relay selection is performed after or before the start of transmission. Specifically, for each relay-selection strategy, we first obtain a closed-form expression for the end-to-end (E2E) error probability with an arbitrary constellation, which accounts for all the resulting nonuniform constellation cases due to constellation rotation. Subsequently, with the derived expressions, we then formulate an optimization problem that considers the joint optimization of the rotation angle and the transmit powers at the end-sources and the relays. The objective of the optimization problem is to minimize the E2E error probability of one of the end-sources, while satisfying a set of total and individual transmit power constraints and a predefined threshold for the E2E error probability of the other end-source. Numerical results verify the theoretical analysis, and show that the scheme proposed herein provides not only higher spectral efficiency, but also more reliable transmission.**

***Index Terms*—Cooperative communication, decode-and-forward, error probability, relay selection, signal space diversity (SSD), time division broadcast (TDBC) protocol, two-way relaying.**

Manuscript received February 25, 2016; revised October 23, 2016; accepted December 12, 2016. Date of publication January 4, 2017; date of current version July 14, 2017. This work was supported in part by Huawei Canada Company Ltd., and in part by the Ontario Ministry of Economic Development and Innovation's ORF-RE (Ontario Research Fund-Research Excellence) program. This paper was presented in part at the IEEE Global Communications Conference, San Diego, CA, USA, December 2015. The review of this paper was coordinated by Dr. L. Zhao.

H. U. Sokun, M. C. Ilter, and H. Yanikomeroglu are with the Department of Systems and Computer Engineering, Carleton University, Ottawa, ON K1S 5B6, Canada (e-mail: husokun@sce.carleton.ca; ilterm@sce.carleton.ca; halim@sce.carleton.ca).

S. Ikki is with the Department of Electrical Engineering, Lakehead University, Thunder Bay, ON P7B 5E1, Canada (e-mail: sikki@lakeheadu.ca).

Color versions of one or more of the figures in this paper are available online at http://ieeexplore.ieee.org.

Digital Object Identifier 10.1109/TVT.2017.2647813

I. Introduction

Mobile data traffic growth is increasing at an accelerating rate, which is driven by the proliferation of smartphones and data services. To meet the growth in data traffic and provide ubiquitous mobile broadband coverage, relay aided communication has been recognized as an important enabler. This technology has been used by several recent standards such as 3GPP LTE-Advanced, IEEE 802.16j, and IEEE 802.16m [2], and it is also a promising technology for future 5G communications [3].

The traditional relay system model, i.e., one-way relaying, consists of three nodes: a source node, a destination node, and a relay node. In this system model, the source communicates with the destination through an intermediate relay, and spatial diversity is exploited by combining the signals from the source-destination and relay-destination links. To improve the spatial diversity gain in the system, multiple relays can be incorporated into this model. However, such a model enables spatial diversity at the expense of spectral efficiency [4] due to half-duplex operation[1] and the need of orthogonal time (or frequency) slots to transmit messages.

To diminish the loss in spectral efficiency and achieve the desired network performance, two-way relaying has been introduced in [6] and [7]; it allows transmission of two simultaneous flows rather than a single one. There are two well-known protocols for decode-and-forward (DF) two-way relaying: physical-layer network coding (PNC) [6] and time division broadcast protocol (TDBC) [7]. To execute exchange of information between the end-sources, TDBC requires three time slots, whereas PNC needs two time slots. It is obvious that TDBC is a less efficient protocol in comparison to PNC since it needs more time slots than PNC to fulfill message exchange. However, TDBC provides more reliability than PNC since it exploits direct link between the end-sources.

In addition to two-way relaying, an effective technique, the so-called best-relay selection [8], can be used to overcome the spectrum inefficiency. In this technique, only a single relay among the candidate relays is chosen based on a certain

[1] The reduction in spectral efficiency due to half-duplex relaying may be overcome by full-duplex relaying. However, even though full-duplex transmission is a promising duplexing mechanism that offers numerous benefits for increasing spectral efficiency, these potential benefits are accompanied with a number of challenges at all layers [5]. Discussing the advantages/disadvantages of half-duplex and full-duplex systems, or comparing these two systems with each other is beyond the scope of this paper.

strategy to retransmit the end-sources' messages. For the best-relay selection, two typical strategies are considered: reactive and proactive relay selections. In a reactive mode, the best relay among the relays that successfully detect the messages in the first and second time slots is allowed to participate in cooperation, whereas in a proactive mode, a specific relay that is selected prior to both the end-sources' transmission participates in cooperation. For choosing the best candidate, the proactive strategy needs global channel state information (CSI) at the first and second hops, whereas the reactive strategy only needs local CSI at the second hops. Hence, the reactive strategy requires less signaling overhead than the proactive one. However, the latter is more energy efficient since only a single relay overhears the transmitted messages in the first and second time slots [9], [10].

The efficiency with which spectrum is used can be further enhanced by utilizing signal space diversity (SSD) technique [11] along with relay selection and two-way relaying. The SSD technique exploits the diversity in the modulation signal space as follows: First, original data symbols are rotated by a certain angle prior to transmission. Next, in-phase and quadrature-phase interleaving is employed to the rotated symbols to ensure that in-phase and quadrature-phase components are sent over independent realizations of the channel.

The SSD technique has been already considered in one-way relaying [12]–[17]. For instance, in a single DF relaying system, the end-to-end (E2E) error performance analysis of the SSD technique has been investigated over both Rayleigh fading [12], [13] and Nakagami-m fading channels [14]. In addition, the outage analysis of the single DF relaying system with the SSD technique has been studied over Nakagami-m fading channels [15]. On the other hand, in [16] and [17], the E2E error performance of the SSD technique along with the best-relay selection has been discussed in multirelay DF relaying systems. However, to the best of authors' knowledge, the performance of the SSD technique has not yet been investigated in two-way relaying systems with the best-relay selection approach.

A. Contribution

In this paper, we introduce a novel transmission scheme that jointly considers the SSD technique, the TDBC protocol, and the best-relay selection. Such a scheme enables to achieve a higher spectral efficiency, and at the same time to provide a higher reliability in transmission. In particular, the contributions of the paper are the following:

1) We obtain a closed-form expression for the probability density function (PDF) of the output signal-to-noise ratio (SNR) at the end-sources when both the reactive and proactive relay-selection strategies are considered.

2) A closed-form expression for the E2E error probability with an arbitrary two-dimensional (2-D) constellation is obtained for both the reactive and proactive relay-selection strategies, which is tight and accounts for all nonuniform constellation cases that are caused by constellation rotation. The derived expressions allow choosing the best rotation angle as a function of SNR, and optimizing the rotation angle and the transmit powers of all nodes jointly.

3) Hence, utilizing these expressions, and considering that all transmitting nodes have equal power, we first determine the optimum rotation angle at different SNR values to minimize the E2E error probability of one of the end-source while meeting a predetermined threshold for the E2E error probability of the other end-source.

4) Then, we perform joint optimization of rotation angle and transmit power allocation at different SNR values to minimize the E2E error probability of one of the end-sources while maintaining the total and the individual transmit power constraints and a predetermined threshold for the E2E error probability of the other end-source.

5) The analytical results are corroborated through Monte Carlo simulations.

B. Outline

The rest of the paper is structured as follows. Section II describes the adopted system and channel models and introduces the considered protocol. In Section III, the closed-form expression of the E2E error probability is obtained for the cases when reactive and proactive relay-selection strategies are considered. In Section IV, considering the different relay-selection strategies, the system optimization is carried out for two different objectives: single optimization of rotation angle when all transmitting nodes have the same power and joint optimization of both rotation angle and transmit power allocation. Finally, the simulation results are presented in Section V and concluding remarks are provided in Section VI.

II. Preliminaries and Assumptions

A. System and Channel Models

The system under consideration consists of two end-sources ($\mathcal{A}$ and $\mathcal{B}$) and L intermediate relays ($\mathcal{R}_1, \ldots, \mathcal{R}_\ell, \ldots, \mathcal{R}_L$). In this system, two end-sources exchange information through one out of the L relays over independent nonidentically distributed Rayleigh fading channels. Considering that the channels are reciprocal,[2] the circularly symmetric complex Gaussian channel gains of the links $\mathcal{A} \rightarrow \mathcal{R}_\ell$, $\mathcal{B} \rightarrow \mathcal{R}_\ell$, and $\mathcal{A} \rightarrow \mathcal{B}$ are denoted by $h_{\mathcal{A}\mathcal{R}_\ell} \sim \mathcal{N}(0, \Omega_{\mathcal{A}\mathcal{R}_\ell})$, $h_{\mathcal{B}\mathcal{R}_\ell} \sim \mathcal{N}(0, \Omega_{\mathcal{B}\mathcal{R}_\ell})$, and $h_{\mathcal{A}\mathcal{B}} \sim \mathcal{N}(0, \Omega_{\mathcal{A}\mathcal{B}})$, respectively. Moreover, the additive white Gaussian noise terms of all links are assumed to have zero-mean and equal variance (N_0).

B. SSD-Based TDBC in Two-Way Relaying Systems

To enhance both the performance and spectral efficiency of the system, we consider combining the SSD technique with TDBC protocol (the so-called SSD-based TDBC protocol). In the conventional TDBC protocol [7], the transmission of two symbols needs three time slots, where the end-source $\mathcal{A}$ and the end-source $\mathcal{B}$ transmit to ℓ-th relay $\mathcal{R}_\ell$ over the first and second time slots, respectively, and in the third time slot, the ℓ-th relay $\mathcal{R}_\ell$ transmits a function of the received signals to the end-source $\mathcal{A}$ and the end-source $\mathcal{B}$.

[2]We consider a time division duplex system where channel reciprocity holds.

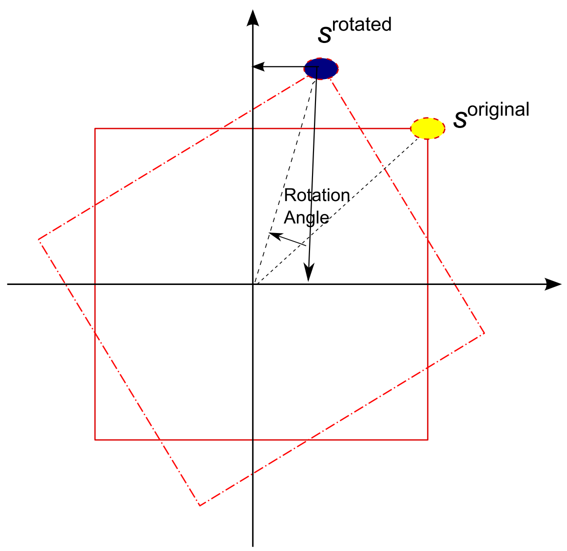

Fig. 1. Example of rotated constellation that is generated by applying a transformation Θ to the quadrature phase shift keying (QPSK) constellation.

However, using SSD-based TDBC protocol, the number of symbols that are transmitted over three time slots can be doubled, i.e., four symbols over three time slots. The basic idea behind SSD-based TDBC protocol is that the original symbols are rotated by a certain angle before being transmitted from both the end-sources $\mathcal{A}$ and $\mathcal{B}$, and then, the end-sources $\mathcal{A}$ and $\mathcal{B}$ cooperate with the ℓ-th relay $\mathcal{R}_\ell$ to send the real and imaginary parts of the rotated symbols. In the 2-D signal space, there exists rotations in which the in-phase component and the quadrature component of the transmitted signal carry enough information to uniquely represent the original signal [12].

Let χ be a constellation generated by applying a transformation Θ to an ordinary constellation shown in Fig. 1, and the transformation Θ be given as

$$\Theta = \begin{bmatrix} \cos(\theta) & -\sin(\theta) \\ \sin(\theta) & \cos(\theta) \end{bmatrix}, \tag{1}$$

where θ is the rotation angle in 2-D signal space.

Then, let us assume that $\boldsymbol{s}^{\mathcal{A}} = (s_1^{\mathcal{A}}; s_2^{\mathcal{A}})$ be a pair of signal points from the rotated constellation, i.e., $s_1^{\mathcal{A}}, s_2^{\mathcal{A}} \in \chi$, which corresponds to the end-source $\mathcal{A}$'s message. Note that $s_1^{\mathcal{A}} = \Re\{s_1^{\mathcal{A}}\} + \mathrm{j}\Im\{s_1^{\mathcal{A}}\}$ and $s_2^{\mathcal{A}} = \Re\{s_2^{\mathcal{A}}\} + \mathrm{j}\Im\{s_2^{\mathcal{A}}\}$, where $\Re\{.\}$ and $\Im\{.\}$ represent the in-phase and the quadrature components of the corresponding signal points, respectively. After interleaving the components of $s_1^{\mathcal{A}}$ and $s_2^{\mathcal{A}}$, the new constellation point that will be sent from the end-source $\mathcal{A}$ can be written as

$$\lambda_{\mathcal{A}} = \Re\{s_1^{\mathcal{A}}\} + \mathrm{j}\Im\{s_2^{\mathcal{A}}\}. \tag{2}$$

Let us next assume that $\boldsymbol{s}^{\mathcal{B}} = (s_1^{\mathcal{B}}; s_2^{\mathcal{B}})$ be a pair of signal points from the rotated constellation, i.e., $s_1^{\mathcal{B}}, s_2^{\mathcal{B}} \in \chi$, which corresponds to the end-source $\mathcal{B}$'s message. Similar to the end-source $\mathcal{A}$, the constellation point that will be transmitted from the end-source $\mathcal{B}$ is formed by interleaving the components of $s_1^{\mathcal{B}}$ and $s_2^{\mathcal{B}}$ as follows:

$$\lambda_{\mathcal{B}} = \Re\{s_1^{\mathcal{B}}\} + \mathrm{j}\Im\{s_2^{\mathcal{B}}\}. \tag{3}$$

It is worth mentioning that both $\lambda_{\mathcal{A}}$ and $\lambda_{\mathcal{B}}$ do not belong to the rotated constellation any more; rather, they belong to the expanded constellation, Λ, defined as

$$\Lambda = \Re\{\chi\} \times \Im\{\chi\}, \tag{4}$$

where $\times$ denotes the Cartesian product of two sets. In this expanded constellation, all members consist of two components each of which uniquely identifies a particular member of χ. Thus, decoding a member of the expanded constellation results in decoding two different members of the original constellation.

In the first time slot, the received signals at the end-source $\mathcal{B}$ and the ℓ-th relay $\mathcal{R}_\ell$ can be written as

$$y^{\mathcal{A}\to\mathcal{B}} = h_{\mathcal{A}\mathcal{B}}\sqrt{P_{\mathcal{A}}}\lambda_{\mathcal{A}} + n_{\mathcal{B}}, \tag{5}$$

$$y^{\mathcal{A}\to\mathcal{R}_\ell} = h_{\mathcal{A}\mathcal{R}_\ell}\sqrt{P_{\mathcal{A}}}\lambda_{\mathcal{A}} + n_{\mathcal{R}_\ell}, \tag{6}$$

where $P_{\mathcal{A}}$ denotes the transmit power at the end-source $\mathcal{A}$.

In the second time slot, the received signals at the end-source $\mathcal{A}$ and the ℓ-th relay $\mathcal{R}_\ell$ can be given as

$$y^{\mathcal{B}\to\mathcal{A}} = h_{\mathcal{A}\mathcal{B}}\sqrt{P_{\mathcal{B}}}\lambda_{\mathcal{B}} + n_{\mathcal{A}}, \tag{7}$$

$$y^{\mathcal{B}\to\mathcal{R}_\ell} = h_{\mathcal{B}\mathcal{R}_\ell}\sqrt{P_{\mathcal{B}}}\lambda_{\mathcal{B}} + \tilde{n}_{\mathcal{R}_\ell}, \tag{8}$$

where $P_{\mathcal{B}}$ denotes the transmit power at the end-source $\mathcal{B}$.

The detection of the end-sources' signals at the ℓ-th relay, i.e., $s_1^{\mathcal{A}}$ and $s_2^{\mathcal{A}}$ from $\lambda_{\mathcal{A}}$, and $s_1^{\mathcal{B}}$ and $s_2^{\mathcal{B}}$ from $\lambda_{\mathcal{B}}$, is given as

$$\hat{\lambda}_{\mathcal{A}} = \arg\min_{\lambda_{\mathcal{A}}\in\Lambda}\left[y^{\mathcal{A}\to\mathcal{R}_\ell} - h_{\mathcal{A}\mathcal{R}_\ell}\sqrt{P_{\mathcal{A}}}\lambda_{\mathcal{A}}\right], \tag{9}$$

$$\hat{\lambda}_{\mathcal{B}} = \arg\min_{\lambda_{\mathcal{B}}\in\Lambda}\left[y^{\mathcal{B}\to\mathcal{R}_\ell} - h_{\mathcal{B}\mathcal{R}_\ell}\sqrt{P_{\mathcal{B}}}\lambda_{\mathcal{B}}\right]. \tag{10}$$

It is important to note that knowing $\lambda_{\mathcal{A}}$ and $\lambda_{\mathcal{B}}$ lead to knowing $(s_1^{\mathcal{A}}, s_2^{\mathcal{A}})$ and $(s_1^{\mathcal{B}}, s_2^{\mathcal{B}})$, respectively.

As shown in Fig. 2, we consider two types of relay-selection strategies: reactive and proactive relay selections. In the reactive mode, only the best is selected to be active among a set of relays that successfully decode the message in the first and second time slots. The set that is formed by the relays that successfully decode the message in the first and second time slots, is called the decoding set, C. For two-way relaying networks, the choice of reactive relay-selection criterion is not trivial since there are two different data transmissions with different error probabilities and SNRs. To increase the reliability in the system, we consider to maximize the minimum SNR of the two end-sources. Hence, the relay, which maximizes the minimum SNR of the two end-sources, in the decoding set C is chosen, that is

$$\mathcal{R}_b = \arg\max_{i\in C}\left[\min\left(\gamma_{\mathcal{A}\mathcal{R}_i}, \gamma_{\mathcal{B}\mathcal{R}_i}\right)\right], \tag{11}$$

where $\gamma_{\mathcal{A}\mathcal{R}_i} = |h_{\mathcal{A}\mathcal{R}_i}|^2 P_{\mathcal{A}}/N_0$ and $\gamma_{\mathcal{B}\mathcal{R}_i} = |h_{\mathcal{B}\mathcal{R}_i}|^2 P_{\mathcal{B}}/N_0$ are the SNRs between the end-source $\mathcal{A}$ and the i-th relay and between the end-source $\mathcal{B}$ and the i-th relay, respectively.

On the other hand, in the proactive mode, we select the relay before sending the data. The selection will be among all the relays since we do not know in advance which relay can detect both users' data correctly. Therefore, the relay, which maximizes the minimum SNR of the two end-sources, among all the relays

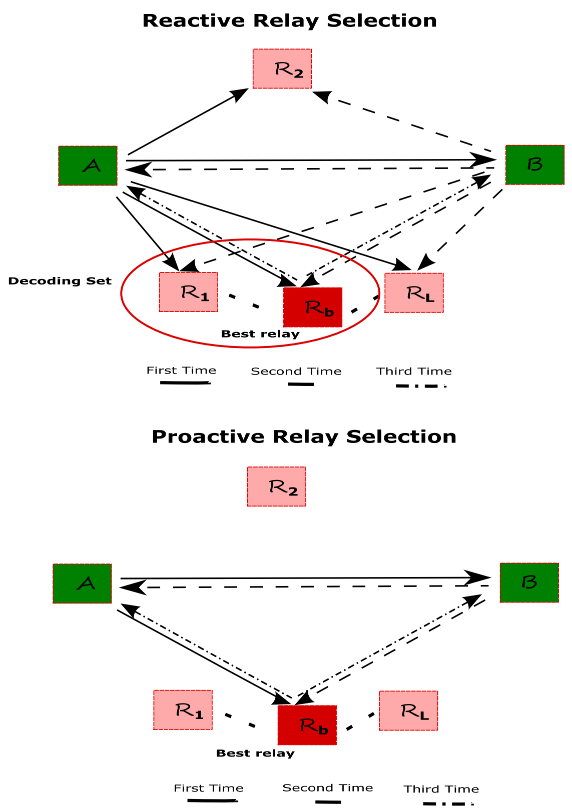

Fig. 2. Illustration of a two-way relaying network with both reactive and proactive relay selections.

is chosen, that is

$$\mathcal{R}_b = \arg\max_{i \in L} \left[\min\left(\gamma_{\mathcal{AR}_i}, \gamma_{\mathcal{BR}_i}\right)\right]. \tag{12}$$

It is important to mention that if this relay detects both signals correctly, the selected relay will be on. Otherwise, the mentioned relay remains silent.

In the third time slot, there can be at most one active relay irrespective of the considered relay-selection strategy. The new constellation point that will be sent from the selected relay, $\mathcal{R}_b$, is formed by interleaving the components of $s_1^{\mathcal{A}}$ and $s_2^{\mathcal{A}}$ and $s_1^{\mathcal{B}}$ and $s_2^{\mathcal{B}}$ as follows:

$$\lambda_{\mathcal{R}_b} = \sqrt{\beta}\left(\Re\{s_2^{\mathcal{A}}\} + \mathrm{j}\Im\{s_1^{\mathcal{A}}\}\right) + \sqrt{1-\beta}\left(\Re\{s_2^{\mathcal{B}}\} + \mathrm{j}\Im\{s_1^{\mathcal{B}}\}\right), \tag{13}$$

where β is a normalization parameter that maintains the average signal power at unity.

The received signals at the end-sources can be given as

$$y^{\mathcal{R}_b \to \mathcal{A}} = h_{\mathcal{AR}_b}\sqrt{P_{\mathcal{R}}}\lambda_{\mathcal{R}_b} + \tilde{n}_{\mathcal{A}}, \tag{14}$$

$$y^{\mathcal{R}_b \to \mathcal{B}} = h_{\mathcal{BR}_b}\sqrt{P_{\mathcal{R}}}\lambda_{\mathcal{R}_b} + \tilde{n}_{\mathcal{B}}, \tag{15}$$

where $P_{\mathcal{R}}$ is the transmit power used in the third time slot.[3]

[3]The transmit power at the relays is $P_{\mathcal{R}_\ell} = P_{\mathcal{R}}$, $\ell = 1, \ldots, L$. As such, $P_{\mathcal{R}}$ is used to represent not only the transmit power of the selected relay but also the transmit power of the other relays. Note that since we consider the relay selection, there can be only one active relay (the best one) in the third time slot, whereas the other relays remain inactive.

Since the end-sources $\mathcal{A}$ and $\mathcal{B}$ know their own data, the backpropagating known data can be cancelled out, and hence, the modified received signals at the end-sources $\mathcal{A}$ and $\mathcal{B}$ can be expressed as

$$y^{\mathcal{R}_b \to \mathcal{A}} = h_{\mathcal{AR}_b}\sqrt{P_{\mathcal{R}}(1-\beta)}\left[\Re\{s_2^{\mathcal{B}}\} + \mathrm{j}\Im\{s_1^{\mathcal{B}}\}\right] + \tilde{n}_{\mathcal{A}}, \tag{16}$$

$$y^{\mathcal{R}_b \to \mathcal{B}} = h_{\mathcal{BR}_b}\sqrt{P_{\mathcal{R}}\beta}\left[\Re\{s_2^{\mathcal{A}}\} + \mathrm{j}\Im\{s_1^{\mathcal{A}}\}\right] + \tilde{n}_{\mathcal{B}}, \tag{17}$$

Considering the direct and the cooperative links, the received signals at the end-source B in the first and third time slots can be given as

$$y^{\mathcal{A} \to \mathcal{B}} = h_{\mathcal{AB}}\sqrt{P_{\mathcal{A}}}\left[\Re\{s_1^{\mathcal{A}}\} + \mathrm{j}\Im\{s_2^{\mathcal{A}}\}\right] + n_{\mathcal{B}}, \tag{18}$$

$$y^{\mathcal{R}_b \to \mathcal{B}} = h_{\mathcal{BR}_b}\sqrt{P_{\mathcal{R}}\beta}\left[\Re\{s_2^{\mathcal{A}}\} + \mathrm{j}\Im\{s_1^{\mathcal{A}}\}\right] + \tilde{n}_{\mathcal{B}}. \tag{19}$$

By comparing the received signals at user $\mathcal{B}$, it is observed that the received signal from the selected relay contains components of the original signal that are not included in the received signal from user $\mathcal{A}$. Hence, from the user $\mathcal{B}$ point of view, different components of each member of the original signal (i.e., $s_1^{\mathcal{A}}$ and $s_2^{\mathcal{A}}$), are affected by independent channel fading.

To detect the original message, the end-source $\mathcal{B}$ reorders the received components so that the corresponding components of each signal point in $\boldsymbol{s}^{\mathcal{A}}$ join together. Let $\boldsymbol{r}^{\mathcal{A}\to\mathcal{B}} = (r_1^{\mathcal{A}\to\mathcal{B}}; r_2^{\mathcal{A}\to\mathcal{B}}; r_3^{\mathcal{A}\to\mathcal{B}}; r_4^{\mathcal{A}\to\mathcal{B}})$ be the end-source $\mathcal{B}$'s signal after reordering the received components [17]. Thus

$$r_1^{\mathcal{A}\to\mathcal{B}} = \Re\{h_{\mathcal{AB}}^* y^{\mathcal{A}\to\mathcal{B}}\} = |h_{\mathcal{AB}}|^2\sqrt{P_{\mathcal{A}}}\Re\{s_1^{\mathcal{A}}\} + \hat{n}_{\mathcal{B}_1}, \tag{20a}$$

$$r_2^{\mathcal{A}\to\mathcal{B}} = \Im\{h_{\mathcal{AB}}^* y^{\mathcal{A}\to\mathcal{B}}\} = |h_{\mathcal{AB}}|^2\sqrt{P_{\mathcal{A}}}\Im\{s_2^{\mathcal{A}}\} + \hat{n}_{\mathcal{B}_2}, \tag{20b}$$

$$r_3^{\mathcal{A}\to\mathcal{B}} = \Re\{h_{\mathcal{BR}_b}^* y^{\mathcal{R}_b\to\mathcal{B}}\} = |h_{\mathcal{BR}_b}|^2\sqrt{P_{\mathcal{R}}\beta}\Re\{s_2^{\mathcal{A}}\} + \hat{n}_{\mathcal{B}_3}, \tag{20c}$$

$$r_4^{\mathcal{A}\to\mathcal{B}} = \Im\{h_{\mathcal{BR}_b}^* y^{\mathcal{R}_b\to\mathcal{B}}\} = |h_{\mathcal{BR}_b}|^2\sqrt{P_{\mathcal{R}}\beta}\Im\{s_1^{\mathcal{A}}\} + \hat{n}_{\mathcal{B}_4}, \tag{20d}$$

where $\hat{n}_{\mathcal{B}_1}$, $\hat{n}_{\mathcal{B}_2}$, $\hat{n}_{\mathcal{B}_3}$, and $\hat{n}_{\mathcal{B}_4}$ are additive noise components.

The end-source $\mathcal{B}$ applies a maximum likelihood (ML) detector on the reordered signal to detect the source message. Hence, the end-source $\mathcal{B}$'s ML decision rule can be expressed as follows:

$$\hat{s}_1^{\mathcal{A}} = \arg\min_{s_1^{\mathcal{A}} \in \chi}\left[\left|r_1^{\mathcal{A}\to\mathcal{B}} - |h_{\mathcal{AB}}|^2\sqrt{P_{\mathcal{A}}}\Re\{s_1^{\mathcal{A}}\}\right|^2 + \left|r_4^{\mathcal{A}\to\mathcal{B}} - |h_{\mathcal{BR}_b}|^2\sqrt{P_{\mathcal{R}}\beta}\Im\{s_1^{\mathcal{A}}\}\right|^2\right], \tag{21}$$

$$\hat{s}_2^{\mathcal{A}} = \arg\min_{s_2^{\mathcal{A}} \in \chi}\left[\left|r_2^{\mathcal{A}\to\mathcal{B}} - |h_{\mathcal{AB}}|^2\sqrt{P_{\mathcal{A}}}\Im\{s_2^{\mathcal{A}}\}\right|^2 + \left|r_3^{\mathcal{A}\to\mathcal{B}} - |h_{\mathcal{BR}_b}|^2\sqrt{P_{\mathcal{R}}\beta}\Re\{s_2^{\mathcal{A}}\}\right|^2\right]. \tag{22}$$

Following the same procedure, the detection at the end-source $\mathcal{A}$ can be obtained in a similar manner.

Finally, we should mention that there is a scenario in which the relay cannot detect the end-sources' messages correctly. In this situation, both end-sources rely on the direct link only to detect both signals using the expanded constellation. So, the ML detection rule at the end-source $\mathcal{B}$ can be written as

$$\hat{\lambda}_{\mathcal{A}} = \arg\min_{\lambda_{\mathcal{A}}\in\Lambda} \left[y^{\mathcal{A}\to\mathcal{B}} - \sqrt{P_{\mathcal{A}}}h_{\mathcal{AB}}\lambda_{\mathcal{A}}\right]. \quad (23)$$

It is obvious that knowing $\lambda_{\mathcal{A}}$ leads to knowing $s_1^{\mathcal{A}}$ and $s_2^{\mathcal{A}}$. The same rule can be applied at the end-source $\mathcal{A}$. Noting that the proposed protocol doubles the spectral efficiency in the system by sending four symbols in three time slots rather than two symbols in three time slots.

III. E2E Error Probability Performance Analysis

In this section, for both the reactive and proactive relay-selection strategies, we obtained the E2E error probabilities of arbitrary 2-D constellations (as a function of SNR), which accounts for all nonuniform constellations caused by constellation rotation.

A. Reactive Relay-Selection Case

Here, we aim to derive the E2E error probability for the reactive relay-selection case.[4] The E2E error probability[5] at the j-th end-source can be expressed as

$$\begin{aligned}\overline{P}_j(e) \;=\; & \Pr[C_0=\emptyset]\overline{P}^{i\to j}_{\text{direct}} + \sum_{m=1}^{2^L-1}\Pr[C_m] \\ & \times\sum_{i=1}^{|C_m|}\Pr\left[\mathcal{R}_b=\mathcal{R}_i|C_m\right]\overline{P}^{i\to\mathcal{R}_i\to j}_{\text{coop}}(e\,|\mathcal{R}_b=\mathcal{R}_i, C_m), \\ & i\neq j,\; i,j\in\{\mathcal{A},\mathcal{B}\},\end{aligned} \quad (24)$$

where $\Pr[C_0=\emptyset]$ denotes that none of the relays decode both end-sources' messages correctly, $\Pr[C_m]$ shows the probability of having a decoding set C_m with the cardinality of $|C_m|$, and $\Pr[\mathcal{R}_b=\mathcal{R}_i|C_m]$ is the probability that any relay $\mathcal{R}_i$ can be the best relay $\mathcal{R}_b$ out of a decoding set C_m based on the reactive relay-selection rule given in (11), $\overline{P}^{i\to j}_{\text{direct}}$ is the error probability of the direct link between the end-sources, and also, $\overline{P}^{i\to\mathcal{R}_i\to j}_{\text{coop}}(e|\mathcal{R}_b=\mathcal{R}_i, C_m)$ gives the error probability of the cooperation case where the best relay $\mathcal{R}_b$ remains active at the third time slot operation.

1) Calculation of $\overline{P}^{i\to j}_{direct}$: In a direct link scenario, e.g., $\mathcal{A}\to\mathcal{B}$, the end-source $\mathcal{A}$ transmits the symbols selected from the expanded M^2-ary constellation Λ to the end-source $\mathcal{B}$ with the transmit power $P_{\mathcal{A}}$. Thus, the received instantaneous SNR at end-source $\mathcal{B}$ can be given by $\gamma_{\mathcal{B}}^{\text{direct}} = P_{\mathcal{A}}|h_{\mathcal{AB}}|^2/N_0$. Then, the instantaneous error probability expression at end-source $\mathcal{B}$ can be written in the form of a function of $\gamma_{\mathcal{B}}^{\text{direct}}$

$$\begin{aligned}&\overline{P}^{\mathcal{A}\to\mathcal{B}}_{\text{direct}}\left(\gamma_{\mathcal{B}}^{\text{direct}}\right) \\ &= \sum_{k=0}^{M^2-1}\sum_{\substack{l=0\\ l\neq k}}^{M^2-1}\mathsf{P}_k\Pr\left[y^{\mathcal{A}\to\mathcal{B}}\in D_{\Lambda(l)}\left(\gamma_{\mathcal{B}}^{\text{direct}}\right)|\lambda_{\mathcal{A}}=\Lambda(k)\right],\end{aligned} \quad (25)$$

where P_k is the probability of transmitting the k-th symbol, $\Lambda(k)$ is the k-th symbol in the expanded constellation, and $D_{\Lambda(k)}$ is the decision region of the symbol $\Lambda(k)$. Note that $\overline{P}^{\mathcal{A}\to\mathcal{B}}_{\text{direct}}$ consists of the sum all possibilities that the transmitted $\Lambda(l)$ symbol drops into $D_{\Lambda(k)}$. For equiprobable signaling case, $\mathsf{P}_k = 1/M^2$, $D_{\Lambda(k)}$ can be expressed as [18]

$$D_{\Lambda(k)}\left(\gamma_{\mathcal{B}}^{\text{direct}}\right) = \left\{\begin{matrix} y^{\mathcal{A}\to\mathcal{B}} : \mathcal{L}_{k,l}\left(\frac{y^{\mathcal{A}\to\mathcal{B}}}{h_{\mathcal{AB}}}\right) < 0, \\ l\neq k, l=0,\ldots,M^2-1\end{matrix}\right\}, \quad (26)$$

where

$$\mathcal{L}_{k,l}\left(y^{\mathcal{A}\to\mathcal{B}}\right) = \Re\left[y^{\mathcal{A}\to\mathcal{B}}c^*_{k,l}\right] + d_{k,l}, \quad (27a)$$

$$c_{k,l} = \Lambda(l) - \Lambda(k), \quad (27b)$$

$$d_{k,l} = \frac{1}{2}\left[|\Lambda(k)|^2 - |\Lambda(l)|^2\right]. \quad (27c)$$

In the upcoming steps, $\mathcal{L}_{k,l}(y^{\mathcal{A}\to\mathcal{B}})$ is replaced with $\bar{\mathcal{L}}_{k,l}(y^{\mathcal{A}\to\mathcal{B}})$, which is a normalized version with respect to $|c_{k,l}|$. By utilizing the geometric trajectory on 2-D space shown in [19], $\Pr[y^{\mathcal{A}\to\mathcal{B}}\in D_{\Lambda(l)}(\gamma_{\mathcal{B}})|\lambda_{\mathcal{A}}=\Lambda(k)]$ can be formulated as

$$\begin{aligned}&\Pr\left[y^{\mathcal{A}\to\mathcal{B}}\in D_{\Lambda(l)}(\gamma_{\mathcal{B}})|\lambda_{\mathcal{A}}=\Lambda(k)\right] \\ &= \sum_{t=1}^{T_l}\pm\,\mathrm{Q}\left(\pm\mathcal{L}_{l,p_t}(\Lambda(k))\sqrt{2\gamma_{\mathcal{B}}}, \pm\mathcal{L}_{l,p_{t+1}}(\Lambda(k))\sqrt{2\gamma_{\mathcal{B}}^{\text{direct}}};\right. \\ &\left.\pm\Re\left[c_{l,p_t}, c^*_{l,p_t}\right]\right),\end{aligned} \quad (28)$$

where T_l denotes the lines bounding the decision region $D_{\Lambda(l)}$. In (28), the neighbor decision regions of the symbol $\Lambda(l)$ are expressed by $\Lambda(p_t)$ and $\Lambda(p_{t+1})$ and $\mathrm{Q}(\cdot,\cdot;\cdot)$ denotes the complementary cumulative density function (CCDF) of a bivariate Gaussian variable [20]. The detailed information about the sign $\pm$ and summation terms can be found in [21].

The $\overline{P}^{\mathcal{A}\to\mathcal{B}}_{\text{direct}}$ can be obtained by taking the average of (25) over $\gamma_{\mathcal{B}}^{\text{direct}}$ as

$$\begin{aligned}\overline{P}^{\mathcal{A}\to\mathcal{B}}_{\text{direct}} &= \mathbb{E}_{\gamma_{\mathcal{B}}^{\text{direct}}}\left[P^{\mathcal{A}\to\mathcal{B}}_{\text{direct}}\left(\gamma_{\mathcal{B}}^{\text{direct}}\right)\right] \\ &= \int_0^\infty P^{\mathcal{A}\to\mathcal{B}}_{\text{direct}}\left(\gamma_{\mathcal{B}}^{\text{direct}}\right) f^{\mathcal{A}\to\mathcal{B}}_{\text{direct}}\left(\gamma_{\mathcal{B}}^{\text{direct}}\right) d\gamma_{\mathcal{B}}^{\text{direct}} \\ &= \sum_{k=0}^{M^2-1}\sum_{\substack{l=0\\ l\neq k}}^{M^2-1}\sum_{t=1}^{T_l}\pm\int_0^\infty \mathrm{Q}(a,b;\rho)\, f^{\mathcal{A}\to\mathcal{B}}_{\text{direct}}\left(\gamma_{\mathcal{B}}^{\text{direct}}\right) d\gamma_{\mathcal{B}}^{\text{direct}},\end{aligned} \quad (29)$$

[4]In practice, there is no need to perform relay selection if channels do not change. Hence, the results provided herein can be considered as an upper bound on the performance. In this paper, we assume that the final decision regarding whether or not to perform relay selection has been made by a higher layer mechanism that optimizes the system performance.

[5]Note that we derive a closed-form expression for the symbol error rate. However, all the analyses given herein can also be modified for the bit error rate by just adding a multiplication term of $\frac{1}{2\log_2 M}d_H(\Lambda(l),\Lambda(k))$ into (25), where $d_H(\cdot)$ is the Hamming distance.

where $a = \pm\bar{\mathcal{L}}_{l,p_t}(\Lambda(k))\sqrt{2\gamma_{\mathcal{B}}^{\text{direct}}}$, $b = \pm\bar{\mathcal{L}}_{l,p_{t+1}}(\Lambda(k))\sqrt{2\gamma_{\mathcal{B}}^{\text{direct}}}$, $\rho = \pm\Re[c_{l,p_t}, c^*_{l,p_t}]$, $\mathbb{E}[\cdot]$ denotes the expectation operator, and $f_{\gamma_{\mathcal{B}}}(\gamma_{\mathcal{B}})$ denotes the PDF of $\gamma_{\mathcal{B}}^{\text{direct}}$. Since the channels are assumed to experience Rayleigh fading, $f_{\text{direct}}^{\mathcal{A}\to\mathcal{B}}(\gamma_{\mathcal{B}}^{\text{direct}})$ can be given as

$$f_{\text{direct}}^{\mathcal{A}\to\mathcal{B}}\left(\gamma_{\mathcal{B}}^{\text{direct}}\right) = \frac{1}{\bar{\gamma}_{\mathcal{B}}^{\text{direct}}}\exp\left(-\frac{\gamma_{\mathcal{B}}^{\text{direct}}}{\bar{\gamma}_{\mathcal{B}}^{\text{direct}}}\right), \tag{30}$$

where the average SNR at the end-source $\mathcal{B}$ is $\bar{\gamma}_{\mathcal{B}}^{\text{direct}} = P_{\mathcal{A}}\Omega_{\mathcal{AB}}/N_0$.

The resulting $\overline{P}_{\text{direct}}^{\mathcal{A}\to\mathcal{B}}$ can be expressed as

$$\begin{aligned}
\overline{P}_{\text{direct}}^{\mathcal{A}\to\mathcal{B}} &= \sum_{k=0}^{M^2-1}\sum_{\substack{l=0\\ l\neq k}}^{M^2-1}\sum_{t=1}^{T_l}\frac{1}{2\pi}\int_0^{\upsilon(a,b,\rho)}\int_0^{\infty} d\theta d\gamma_{\mathcal{B}}^{\text{direct}}\\
&\times\exp\left(-\frac{a^2}{2\sin^2\theta}\right)\frac{1}{\bar{\gamma}_{\mathcal{B}}}\exp\left(-\frac{\gamma_{\mathcal{B}}^{\text{direct}}}{\bar{\gamma}_{\mathcal{B}}^{\text{direct}}}\right)\\
&+\frac{1}{2\pi}\int_0^{\upsilon(b,a,\rho)}\int_0^{\infty} d\theta d\gamma_{\mathcal{B}}^{\text{direct}}\exp\left(-\frac{b^2}{2\sin^2\theta}\right)\frac{1}{\bar{\gamma}_{\mathcal{B}}}\exp\left(-\frac{\gamma_{\mathcal{B}}^{\text{direct}}}{\bar{\gamma}_{\mathcal{B}}^{\text{direct}}}\right)\\
&= \sum_{k=0}^{M^2-1}\sum_{\substack{l=0\\ l\neq k}}^{M^2-1}\sum_{t=1}^{T_l}\upsilon(\alpha_1,\alpha_2,\rho)+\upsilon(\alpha_2,\alpha_1,\rho)\\
&-\frac{\alpha_1\arctan\left(\sqrt{\frac{\bar{\gamma}_{\mathcal{B}}^{\text{direct}}\alpha_1^2+2}{\bar{\gamma}_{\mathcal{B}}^{\text{direct}}}}\tan\left(\upsilon(\alpha_1,\alpha_2,\rho)\right)\right)}{\sqrt{\frac{\bar{\gamma}_{\mathcal{B}}^{\text{direct}}\alpha_1^2+2}{\bar{\gamma}_{\mathcal{B}}^{\text{direct}}}}}\\
&-\frac{\alpha_2\arctan\left(\sqrt{\frac{\bar{\gamma}_{\mathcal{B}}^{\text{direct}}\alpha_2^2+2}{\bar{\gamma}_{\mathcal{B}}^{\text{direct}}}}\tan\left(\upsilon(\alpha_2,\alpha_2,\rho)\right)\right)}{\sqrt{\frac{\bar{\gamma}_{\mathcal{B}}^{\text{direct}}\alpha_2^2+2}{\bar{\gamma}_{\mathcal{B}}^{\text{direct}}}}},
\end{aligned}\tag{31}$$

where $\arctan(\cdot)$ represents the inverse of the tangent function, $\alpha_1 = \sqrt{2}\mathcal{L}_{l,p_t}(\Lambda(k))$, $\alpha_2 = \sqrt{2}\mathcal{L}_{l,p_t+1}(\Lambda(k))$ and $\upsilon(\alpha_1,\alpha_2,\rho)$ is defined by

$$\upsilon(\alpha_1,\alpha_2,\rho) = \begin{cases}\arctan\left(\frac{\alpha_1\sqrt{1-\rho^2}}{\alpha_2-\rho\alpha_1}\right), & \rho\alpha_1\leq\alpha_2\\ \arctan\left(\frac{\alpha_1\sqrt{1-\rho^2}}{\alpha_2-\rho\alpha_1}\right)+\pi, & \alpha_2<\rho\alpha_1\\ \arctan\left(\frac{1+\rho}{1-\rho}\right), & \alpha_1=0,\ \alpha_2=0.\end{cases} \tag{32}$$

2) Calculation of $\Pr[C_m]$*:* The probability of having any decoding set, C_m can be written as

$$\Pr[C_m] = \left(\prod_{\kappa_o\notin C_m}\overline{P}_{\text{off},\kappa_o}\right)\left(\prod_{\kappa_i\in C_m}\left(1-\overline{P}_{\text{off},\kappa_i}\right)\right), \tag{33}$$

where

$$\overline{P}_{\text{off},\kappa} = 1-\left(1-\overline{P}_{\text{direct}}^{\mathcal{A}\to\mathcal{R}_\kappa}\right)\left(1-\overline{P}_{\text{direct}}^{\mathcal{B}\to\mathcal{R}_\kappa}\right). \tag{34}$$

Here, $\overline{P}_{\text{direct}}^{\mathcal{A}\to R_\kappa}$ and $\overline{P}_{\text{direct}}^{\mathcal{B}\to R_\kappa}$ correspond to the error probability for the direct links between the end-sources and κ-th relay, which can be obtained from (31).

3) Calculation of $\Pr[\mathcal{R}_b = \mathcal{R}_i|C_m]$*:* Let $\mathcal{Z}_i$ represent the bottleneck term in (11), where $\mathcal{Z}_i = \min(\gamma_{\mathcal{A}\to\mathcal{R}_i}, \gamma_{\mathcal{B}\to\mathcal{R}_i})$. It can be seen that $\mathcal{Z}_i$ is another exponential random variable, and its PDF is given as

$$f_{\mathcal{Z}_i}(z) = \frac{1}{\overline{\mathcal{Z}_i}}\exp\left(-\frac{z}{\overline{\mathcal{Z}_i}}\right), \tag{35}$$

where $\overline{\mathcal{Z}_i} = \overline{\gamma}_{\mathcal{AR}_i} + \overline{\gamma}_{\mathcal{BR}_i}$, $\overline{\gamma}_{\mathcal{AR}_i} = \Omega_{\mathcal{AR}_i}P_{\mathcal{A}}/N_0$, and $\overline{\gamma}_{\mathcal{BR}_i} = \Omega_{\mathcal{BR}_i}P_{\mathcal{B}}/N_0$. It is known that for a given exponential random variable set $\mathcal{Z}_1,\ldots,\mathcal{Z}_{|C_m|}$, the probability of $\mathcal{Z}_i$ being the minimum in this set, can be given as [22]

$$\Pr[\mathcal{Z}_i \text{ is minimum}] = \frac{\overline{\mathcal{Z}}_i}{\sum_{j=1}^{|C_m|}\overline{\mathcal{Z}}_j}. \tag{36}$$

Therefore, the probability that a particular relay can be the best one within a given decoding set can be calculated by utilizing the order statistics of exponential random variable given in (36). For instance, the probability of $\mathcal{Z}_3$ being the maximum in a given set of $\{\mathcal{Z}_1,\mathcal{Z}_2,\mathcal{Z}_3\}$ can be obtained from

$$\begin{aligned}\Pr[\mathcal{Z}_3 \text{ is maximum}] = &\frac{\overline{\mathcal{Z}}_1}{\overline{\mathcal{Z}}_1+\overline{\mathcal{Z}}_2+\overline{\mathcal{Z}}_3}\frac{\overline{\mathcal{Z}}_2}{\overline{\mathcal{Z}}_2+\overline{\mathcal{Z}}_3}\\ &+\frac{\overline{\mathcal{Z}}_2}{\overline{\mathcal{Z}}_1+\overline{\mathcal{Z}}_2+\overline{\mathcal{Z}}_3}\frac{\overline{\mathcal{Z}}_1}{\overline{\mathcal{Z}}_1+\overline{\mathcal{Z}}_3},\end{aligned} \tag{37}$$

where the first term corresponds to the case of $\overline{\mathcal{Z}}_1 < \overline{\mathcal{Z}}_2 < \overline{\mathcal{Z}}_3$ and the second one $\overline{\mathcal{Z}}_2 < \overline{\mathcal{Z}}_1 < \overline{\mathcal{Z}}_3$.

4) Calculation of $\overline{P}_{coop}^{i\to\mathcal{R}_i\to j}(e|\mathcal{R}_b = \mathcal{R}_i, C_m)$*:* In the cooperative scenario, the error probability of the cooperative link, e.g., $\mathcal{A}\to\mathcal{R}_i\to\mathcal{B}$, can be found as

$$\begin{aligned}&\overline{P}_{\text{coop}}^{\mathcal{A}\to\mathcal{R}_b\to\mathcal{B}}(e|\mathcal{R}_b=\mathcal{R}_i, C_m)\\ &= \mathbb{E}_{\gamma_B^{\text{coop}}}\left[P_{\text{coop}}^{\mathcal{A}\to\mathcal{R}_b\to\mathcal{B}}(e|\mathcal{R}_b=\mathcal{R}_i, C_m)\right]\\ &\approx \sum_{k=0}^{M-1}\sum_{\substack{l=0\\ l\neq k}}^{M-1}\sum_{t=1}^{T_l}\pm\int_0^{\infty}\mathrm{Q}(a,b;\rho)\, f_{\gamma_B^{\text{coop}}}^{\mathcal{A}\to\mathcal{R}_i\to\mathcal{B}}(\gamma)\,d\gamma,\end{aligned} \tag{38}$$

where

$$\gamma_B^{\text{coop}} = \gamma_{\mathcal{R}_i\mathcal{B}} + \gamma_{\mathcal{AB}}, \tag{39a}$$

$$a = \pm\bar{\mathcal{L}}_{l,p_t}\left(\sqrt{\beta}\chi(k)\right)\sqrt{2\gamma_B^{\text{coop}}}, \tag{39b}$$

$$b = \pm\bar{\mathcal{L}}_{l,p_{t+1}}\left(\sqrt{\beta}\,\chi(k)\right)\sqrt{2\gamma_B^{\text{coop}}}, \tag{39c}$$

$$\rho = \pm\Re\left[c_{l,p_t}, c^*_{l,p_t}\right]. \tag{39d}$$

The PDF of $f_{\gamma_B^{\text{coop}}}^{\mathcal{A}\to\mathcal{R}_i\to\mathcal{B}}(\gamma)$ is a convolution of $f_{\gamma_{\mathcal{R}_i\mathcal{B}}}(\gamma)$ and $f_{\gamma_{\mathcal{AB}}}(\gamma)$, i.e., $f_{\gamma_B^{\text{coop}}}^{\mathcal{A}\to\mathcal{R}_i\to\mathcal{B}}(\gamma) = f_{\gamma_{\mathcal{R}_i\mathcal{B}}}(\gamma) * f_{\gamma_{\mathcal{AB}}}(\gamma)$. The PDF of $\gamma_{\mathcal{R}_i\mathcal{B}}(\gamma)$ and $f_{\gamma_{\mathcal{R}_i\mathcal{B}}}(\gamma)$, can be obtained from the derivative of the joint CDF of $(\mathcal{Z}_i, \gamma_{\mathcal{R}_i\mathcal{B}}(z,\gamma))$ and $F_{\mathcal{Z}_i,\gamma_{\mathcal{R}_i\mathcal{B}}}(z,\gamma)$, which is defined as

$$\begin{aligned} F_{\mathcal{Z}_i,\gamma_{\mathcal{R}_i\mathcal{B}}}(z,\gamma) &= \Pr[\mathcal{Z}_i \le z, \gamma_{\mathcal{R}_i\mathcal{B}} \le \gamma] \\ &= \Pr[\gamma_{\mathcal{AR}_i} > \gamma_{\mathcal{BR}_i}] \Pr[\gamma_{\mathcal{BR}_i} \le z, \gamma_{\mathcal{R}_i\mathcal{B}} \le \gamma | \gamma_{\mathcal{AR}_i} > \gamma_{\mathcal{BR}_i}] \\ &\quad + \Pr[\gamma_{\mathcal{BR}_i} > \gamma_{\mathcal{AR}_i}] \Pr[\gamma_{\mathcal{AR}_i} \le z, \gamma_{\mathcal{R}_i\mathcal{B}} \le \gamma | \gamma_{\mathcal{BR}_i} > \gamma_{\mathcal{AR}_i}]. \end{aligned} \tag{40}$$

By using the order statistics given in (36), $F_{\mathcal{Z}_i,\gamma_{\mathcal{R}_i\mathcal{B}}}(z,\gamma)$ can be rewritten as

$$\begin{aligned} F_{\mathcal{Z}_i,\gamma_{\mathcal{R}_i\mathcal{B}}}(z,\gamma) = &\frac{\overline{\gamma}_{\mathcal{AR}_i}}{\overline{\gamma}_{\mathcal{BR}_i} + \overline{\gamma}_{\mathcal{AR}_i}} F_{\gamma_{\mathcal{AR}_i}}(z) F_{\gamma_{\mathcal{R}_i\mathcal{B}}}(\gamma) \\ &+ \frac{\overline{\gamma}_{\mathcal{BR}_i}}{\overline{\gamma}_{\mathcal{BR}_i} + \overline{\gamma}_{\mathcal{AR}_i}} \Big\{ F_{\gamma_{\mathcal{BR}_i}}(z)\, u(\gamma/\mathcal{K}_{\mathcal{AB}} - z) \\ &+ F_{\gamma_{\mathcal{BR}_i}}(\gamma/\mathcal{K}_{\mathcal{AB}})\, u(z - \gamma/\mathcal{K}_{\mathcal{AB}}) \\ &- F_{\gamma_{\mathcal{BR}_i}}(z)\, \delta(z - \gamma/\mathcal{K}_{\mathcal{AB}}) \Big\}, \end{aligned} \tag{41}$$

where $\overline{\gamma}_{\mathcal{R}_i\mathcal{B}} = \mathcal{K}_{\mathcal{AB}}\overline{\gamma}_{\mathcal{BR}_i}$ and $\mathcal{K}_{\mathcal{AB}} = \beta P_{\mathcal{R}}/P_{\mathcal{B}}$. Herein, $u(\cdot)$ and $\delta(\cdot)$ denote the unit step function and dirac delta function, respectively. After using the identity $F_{\gamma_{\mathcal{R}_i\mathcal{B}}}(\gamma) = \lim_{z\to\infty} F_{\mathcal{Z}_i,\gamma_{\mathcal{R}_i\mathcal{B}}}(z,\gamma)$ and taking the derivative of $F_{\gamma_{\mathcal{R}_i\mathcal{B}}}(\gamma)$ with respect to γ, the PDF of $\gamma_{\mathcal{R}_i\mathcal{B}}$ can be obtained as

$$\begin{aligned} f_{\gamma_{\mathcal{R}_i\mathcal{B}}}(\gamma) = &\frac{\overline{\gamma}_{\mathcal{AR}_i}}{\overline{\gamma}_{\mathcal{BR}_i} + \overline{\gamma}_{\mathcal{AR}_i}} f_{\text{direct}}^{\mathcal{R}_i\to\mathcal{B}}(\gamma) \\ &+ \frac{\overline{\gamma}_{\mathcal{BR}_i}}{\overline{\gamma}_{\mathcal{BR}_i} + \overline{\gamma}_{\mathcal{AR}_i}} \frac{1}{\mathcal{K}_{\mathcal{AB}}} f_{\text{direct}}^{\mathcal{B}\to\mathcal{R}_i}\left(\frac{\gamma}{\mathcal{K}_{\mathcal{AB}}}\right). \end{aligned} \tag{42}$$

Using (30) and (42), the PDF of $\gamma_{\mathcal{B}}^{\text{coop}}$ can be expressed as

$$\begin{aligned} f_{\gamma_{\mathcal{B}}^{\text{coop}}}^{\mathcal{A}\to\mathcal{R}_i\to\mathcal{B}}(\gamma) = &\frac{\overline{\gamma}_{\mathcal{AR}_i}}{\overline{\gamma}_{\mathcal{BR}_i} + \overline{\gamma}_{\mathcal{AR}_i}} \frac{1}{\overline{\gamma}_{\mathcal{AB}} - \overline{\gamma}_{\mathcal{R}_i\mathcal{B}}} \\ &\times \left[\exp\left(\frac{-\gamma}{\overline{\gamma}_{\mathcal{AB}}}\right) - \exp\left(\frac{-\gamma}{\overline{\gamma}_{\mathcal{R}_i\mathcal{B}}}\right)\right] \\ &+ \frac{\overline{\gamma}_{\mathcal{BR}_i}}{\overline{\gamma}_{\mathcal{BR}_i} + \overline{\gamma}_{\mathcal{AR}_i}} \frac{1}{\overline{\gamma}_{\mathcal{AB}} - \mathcal{K}_{\mathcal{AB}}\overline{\gamma}_{\mathcal{BR}_i}} \\ &\times \left[\exp\left(\frac{-\gamma}{\overline{\gamma}_{\mathcal{AB}}}\right) - \exp\left(\frac{-\gamma}{\mathcal{K}_{\mathcal{AB}}\overline{\gamma}_{\mathcal{BR}_i}}\right)\right]. \end{aligned} \tag{43}$$

The resulting $\overline{P}_{\text{coop}}^{\mathcal{A}\to\mathcal{R}_b\to\mathcal{B}}(e|\mathcal{R}_b = \mathcal{R}_i, C_m)$ can be written as follows:

$$\begin{aligned} &\overline{P}_{\text{coop}}^{i\to\mathcal{R}_b\to j}(e|\mathcal{R}_b = \mathcal{R}_i, C_m) \\ &\approx \sum_{k=0}^{M-1} \sum_{\substack{l=0 \\ l\ne k}}^{M-1} \sum_{t=1}^{T_l} \pm [A(v_1,\alpha_1) + A(v_2,\alpha_2)], \end{aligned} \tag{44}$$

where $\alpha_1 = \sqrt{2}\mathcal{L}_{l,p_t}(\sqrt{\beta}\chi(k))$, $\alpha_2 = \sqrt{2}\mathcal{L}_{l,p_t+1}(\sqrt{\beta}\chi(k))$, $v_1 = v(\alpha_1,\alpha_2,\rho)$, $v_2 = v(\alpha_2,\alpha_1,\rho)$, and an auxiliary function $A(v_k,\alpha_k)$ for $k \in \{1,\ 2\}$ is given as

$$\begin{aligned} A(v_k,\alpha_k) = &\frac{1}{2\pi\left(\overline{\gamma}_{\mathcal{AR}_i} + \overline{\gamma}_{\mathcal{BR}_i}\right)} \Big[v_k\left(\overline{\gamma}_{\mathcal{AR}_i} + \overline{\gamma}_{\mathcal{BR}_i}\right) \\ &+ \frac{\alpha_k\overline{\gamma}_{\mathcal{BR}_i} \arctan\left(\sqrt{\alpha_k^2 + 2/(\mathcal{K}_{\mathcal{AB}}\overline{\gamma}_{\mathcal{BR}_i})}\tan(v_k)/\alpha_k\right)}{\left(\mathcal{K}_{\mathcal{AB}}\overline{\gamma}_{\mathcal{BR}_i}\right)^{(-3/2)}\left(\overline{\gamma}_{\mathcal{AB}} - \mathcal{K}_{\mathcal{AB}}\overline{\gamma}_{\mathcal{BR}_i}\sqrt{2 + \alpha_k^2\mathcal{K}_{\mathcal{AB}}\overline{\gamma}_{\mathcal{BR}_i}}\right)} \\ &+ \frac{\alpha_k\overline{\gamma}_{\mathcal{AR}_i} \arctan\left(\sqrt{\alpha_k^2 + 2/(\overline{\gamma}_{\mathcal{R}_i\mathcal{B}})}\tan(v_k)/\alpha_k\right)}{\overline{\gamma}_{\mathcal{R}_i\mathcal{B}}^{(-3/2)}\left(\overline{\gamma}_{\mathcal{AB}} - \overline{\gamma}_{\mathcal{R}_i\mathcal{B}}\right)\sqrt{2 + \alpha_k^2\overline{\gamma}_{\mathcal{R}_i\mathcal{B}}}} \\ &- \frac{\alpha_k\left(\overline{\gamma}_{\mathcal{AB}}\left(\overline{\gamma}_{\mathcal{AR}_i} + \overline{\gamma}_{\mathcal{BR}_i}\right) - \overline{\gamma}_{\mathcal{BR}_i}\left(\mathcal{K}_{\mathcal{AB}}\overline{\gamma}_{\mathcal{AR}_i} + \overline{\gamma}_{\mathcal{R}_i\mathcal{B}}\right)\right)}{\sqrt{2 + \alpha_k^2\overline{\gamma}_{\mathcal{AB}}}\left(\overline{\gamma}_{\mathcal{AB}} - \mathcal{K}_{\mathcal{AB}}\overline{\gamma}_{\mathcal{BR}_i}\right)\left(\overline{\gamma}_{\mathcal{AB}} - \mathcal{K}_{\mathcal{AB}}\overline{\gamma}_{\mathcal{R}_i\mathcal{B}}\right)} \\ &\times \arctan\left(\sqrt{\alpha_k^2 + 2/(\overline{\gamma}_{\mathcal{AB}})}\tan(v_k)/\alpha_k\right)\Big]. \end{aligned} \tag{45}$$

Discussion: To give more insight into the analysis, we consider a simple two-relay scenario. For this scenario, the calculation of the E2E error probability at the end-source B and $\overline{P}_{\mathcal{B}}(e)$, can be found as follows.

1) The possible decoding sets $\{C_m\}$ can be listed as $C_m \in \{\emptyset, \{\mathcal{R}_1\}, \{\mathcal{R}_2\}, \{\mathcal{R}_1,\mathcal{R}_2\}\}$, and the probabilities of all the decoding sets are given below:

$$\Pr[C_0] = \overline{P}_{\text{off},\mathcal{R}_1}\overline{P}_{\text{off},\mathcal{R}_2}, \tag{46a}$$
$$\Pr[C_1] = \overline{P}_{\text{off},\mathcal{R}_1}\left(1 - \overline{P}_{\text{off},\mathcal{R}_2}\right), \tag{46b}$$
$$\Pr[C_2] = \left(1 - \overline{P}_{\text{off},\mathcal{R}_1}\right)\overline{P}_{\text{off},\mathcal{R}_2}, \tag{46c}$$
$$\Pr[C_3] = \left(1 - \overline{P}_{\text{off},\mathcal{R}_1}\right)\left(1 - \overline{P}_{\text{off},\mathcal{R}_2}\right). \tag{46d}$$

2) Utilizing (36), the probability of the best relay-selection based on (11) for each possible decoding set can be listed as

$$\Pr[\mathcal{R}_b = \mathcal{R}_1|C_1] = 1, \tag{47a}$$
$$\Pr[\mathcal{R}_b = \mathcal{R}_2|C_2] = 1, \tag{47b}$$
$$\Pr[\mathcal{R}_b = \mathcal{R}_1|C_3] = \frac{\overline{\gamma}_{\mathcal{BR}_2} + \overline{\gamma}_{\mathcal{AR}_2}}{\overline{\gamma}_{\mathcal{BR}_1} + \overline{\gamma}_{\mathcal{AR}_1} + \overline{\gamma}_{\mathcal{BR}_2} + \overline{\gamma}_{\mathcal{AR}_2}}, \tag{47c}$$
$$\Pr[\mathcal{R}_b = \mathcal{R}_2|C_3] = \frac{\overline{\gamma}_{\mathcal{BR}_1} + \overline{\gamma}_{\mathcal{AR}_1}}{\overline{\gamma}_{\mathcal{BR}_1} + \overline{\gamma}_{\mathcal{AR}_1} + \overline{\gamma}_{\mathcal{BR}_2} + \overline{\gamma}_{\mathcal{AR}_2}}. \tag{47d}$$

3) Finally, considering (31), (34), and (44), the E2E error probability $\overline{P}_{\mathcal{B}}(e)$ can be derived as

$$\begin{aligned} \overline{P}_{\mathcal{B}}(e) &= \Pr[C_0]\overline{P}_{\text{direct}}^{\mathcal{A}\to\mathcal{B}} \\ &+ \Pr[C_1]\Pr[\mathcal{R}_b = \mathcal{R}_1|C_1]\,\overline{P}_{\text{coop}}^{\mathcal{A}\to\mathcal{R}_1\to\mathcal{B}}(e|\mathcal{R}_b = \mathcal{R}_1, C_1) \\ &+ \Pr[C_2]\Pr[\mathcal{R}_b = \mathcal{R}_2|C_2]\,\overline{P}_{\text{coop}}^{\mathcal{A}\to\mathcal{R}_2\to\mathcal{B}}(e|\mathcal{R}_b = \mathcal{R}_2, C_2) \end{aligned}$$

$$+\Pr[C_3]\Big\{\Pr\left[\mathcal{R}_b=\mathcal{R}_1|C_3\right]\overline{P}_{\text{coop}}^{\mathcal{A}\to\mathcal{R}_1\to\mathcal{B}}(e\,|\mathcal{R}_b=\mathcal{R}_1,C_3)$$
$$+\Pr\left[\mathcal{R}_b=\mathcal{R}_2|C_3\right]\overline{P}_{\text{coop}}^{\mathcal{A}\to\mathcal{R}_2\to\mathcal{B}}\left(e\,|\mathcal{R}_b=\mathcal{R}_2,C_3\right)\Big\}. \tag{48}$$

B. Proactive Relay-Selection Case

The E2E error probability for the proactive relay-selection case is presented in this section. It is equal to the average of the error probabilities over two cases: cooperative and noncooperative ones. Due to the nature of the proactive relay selection, the best relay is determined before sending the message at the end-sources, in this case, the E2E error probability expression at the j-th end-source is given by

$$\overline{P}_j\left(e\right)=\overline{P}_{\text{off},R_b}\overline{P}_{\text{direct}}^{i\to j}+\left(1-\overline{P}_{\text{off},R_b}\right)\overline{P}_{\text{coop}}^{i\to\mathcal{R}_b\to j}\left(e\right), \tag{49}$$

where $\overline{P}_{\text{off},R_b}$ denotes the probability of the best relay chosen by (12), which does not decode both the end-sources' messages correctly, and $\overline{P}_{\text{coop}}^{i\to\mathcal{R}_b\to j}(e)$ corresponds to the error probability of the cooperation case where the best relay $\mathcal{R}_b$ remains active at the third time slot operation.

1) Calculation of $\overline{P}_{direct}^{i\to j}$: The direct link error analysis for the proactive relay selection, e.g., $\mathcal{A}\to\mathcal{B}$, is the same as the one for reactive relay selection. Hence, the error probability of the direct link between the end-sources $\overline{P}_{\text{direct}}^{\mathcal{A}\to\mathcal{B}}$ can found from (31).

2) Calculation of $\overline{P}_{off,R_b}$: The probability that the selected best relay R_b cannot decode the messages from both of end-sources' messages correctly, and thus, remains silent in third time slot, is given as

$$\overline{P}_{\text{off},R_b}=1-\left(1-\overline{P}_{\text{direct}}^{\mathcal{A}\to R_b}\right)\left(1-\overline{P}_{\text{direct}}^{\mathcal{B}\to R_b}\right), \tag{50}$$

where $\overline{P}_{\text{direct}}^{i\to R_b}$ is given by

$$\begin{aligned}\overline{P}_{\text{direct}}^{i\to R_b}&=\mathbb{E}_{\gamma_{iR_b}}\left[P_{\text{direct}}^{i\to R_b}\left(\gamma\right)\right]\\&=\int_0^\infty P_{\text{direct}}^{i\to R_b}\left(\gamma\right)f_{\gamma_{i\mathcal{R}_b}}\left(\gamma\right)d\gamma\\&=\sum_{k=0}^{M^2-1}\sum_{\substack{l=0\\l\neq k}}^{M^2-1}\sum_{t=1}^{T_l}\pm\int_0^\infty \mathrm{Q}\left(a,b;\rho\right)f_{\gamma_{i\mathcal{R}_b}}\left(\gamma\right)d\gamma. \end{aligned}\tag{51}$$

Here, $f_{\gamma_{i\mathcal{R}_b}}(\gamma)$ corresponds to the PDF of the link between the best relay R_b and the i-th end-source ($\gamma_{iR_b}=|h_{i\mathcal{R}_b}|^2P_i/N_0$) which is found as

$$f_{\gamma_{i\mathcal{R}_b}}\left(\gamma\right)=\sum_{l=1}^{L}\binom{L}{l}\frac{l\left(-1\right)^{l-1}}{\overline{\gamma}_{i\mathcal{R}_b}}\exp\left(\frac{-l\gamma}{\overline{\gamma}}\right)+\sum_{l=1}^{L}\binom{L}{l}$$
$$\times\frac{l\gamma\left(-1\right)^{l-1}}{\overline{\gamma}_{j\mathcal{R}_b}\left(l\overline{\gamma}_{i\mathcal{R}_b}-\overline{\gamma}\right)}\left(\exp\left(\frac{-\gamma}{\overline{\gamma}_{i\mathcal{R}_b}}\right)-\exp\left(\frac{-l\gamma}{\overline{\gamma}}\right)\right), \tag{52}$$

where $\overline{\gamma}=\overline{\gamma}_{i\mathcal{R}_b}\overline{\gamma}_{j\mathcal{R}_b}/(\overline{\gamma}_{i\mathcal{R}_b}+\overline{\gamma}_{j\mathcal{R}_b})$. The resulting error probability between the best relay and i-th end-source, $\overline{P}_{\text{direct}}^{i\to R_b}$, can be expressed as

$$\overline{P}_{\text{direct}}^{i\to R_b}=\sum_{k=0}^{M^2-1}\sum_{\substack{l=0\\l\neq k}}^{M^2-1}\sum_{t=1}^{T_l}\pm\sum_{\kappa=1}^{2}\sum_{i=1}^{L}\frac{-\binom{L}{i}\left(-1\right)^i\overline{\gamma}}{2\pi\overline{\gamma}_{i\mathcal{R}_b}}$$
$$\times\left(v_\kappa-\alpha_\kappa\arctan\left(\sqrt{\alpha_\kappa^2+\frac{2i}{\overline{\gamma}}}\tan\left(v_\kappa\right)/\alpha_k\right)/\sqrt{\alpha_k+2i/\overline{\gamma}}\right)$$
$$-\sum_{\kappa=1}^{2}\sum_{i=1}^{L}\frac{\binom{L}{i}2\left(-1\right)^i}{\pi\overline{\gamma}_{j\mathcal{R}_b}\left(4i^2\overline{\gamma}_{A,R_b}-4i\overline{\gamma}\right)}\left[iv_\kappa\overline{\gamma}_{i\mathcal{R}_b}-v_\kappa\overline{\gamma}\right.$$
$$-\alpha_\kappa i\overline{\gamma}_{i\mathcal{R}_b}^{1.5}\arctan\left(\sqrt{\alpha_\kappa^2+\frac{2}{\overline{\gamma}_{i\mathcal{R}_b}}}\tan\left(v_\kappa\right)/\alpha_\kappa\right)/\sqrt{2+\alpha_\kappa^2\overline{\gamma}_{i\mathcal{R}_b}}$$
$$\left.+\alpha_\kappa\overline{\gamma}^{1.5}\arctan\left(\sqrt{\alpha_\kappa^2+\frac{2i}{\overline{\gamma}_{i\mathcal{R}_b}}}\tan\left(v_k\right)/\alpha_\kappa\right)/\sqrt{2i+\alpha_\kappa^2\overline{\gamma}}\right]. \tag{53}$$

3) Calculation of $\overline{P}_{coop}^{i\to\mathcal{R}_b\to j}(e)$: In a cooperative scenario, the E2E error probability of the cooperative link, e.g., $\mathcal{A}\to\mathcal{R}_b\to\mathcal{B}$ for the case in which $\mathcal{R}_b$ detects both end-sources' messages correctly, can be given as

$$\begin{aligned}\overline{P}_{\text{coop}}^{\mathcal{A}\to\mathcal{R}_b\to\mathcal{B}}\left(e\right)&=\mathbb{E}_{\gamma_B^{\text{coop}}}\left[P_{\text{coop}}^{\mathcal{A}\to\mathcal{R}_b\to\mathcal{B}}\left(e\right)\right]\\&\approx\sum_{k=0}^{M-1}\sum_{\substack{l=0\\l\neq k}}^{M-1}\sum_{t=1}^{T_l}\pm\int_0^\infty\mathrm{Q}\left(a,b;\rho\right)f_{\gamma_B^{\text{coop}}}^{\mathcal{A}\to\mathcal{R}_b\to\mathcal{B}}\left(\gamma\right)d\gamma,\end{aligned}\tag{54}$$

where $\gamma_B^{\text{coop}}=\gamma_{\mathcal{R}_b\mathcal{B}}+\gamma_{\mathcal{AB}}$, $a=\pm\bar{\mathcal{L}}_{l,p_t}(\sqrt{\beta}\chi(k))\sqrt{2\gamma_{\mathcal{B}}}$, $b=\pm\bar{\mathcal{L}}_{l,p_{t+1}}(\sqrt{\beta}\chi(k))\sqrt{2\gamma_{\mathcal{B}}}$, and $\rho=\pm\Re[c_{l,p_t},c_{l,p_t}^*]$. Similar to the developments in the reactive case, the PDF of $f_{\gamma_B^{\text{coop}}}^{\mathcal{A}\to\mathcal{R}_b\to\mathcal{B}}(\gamma)$ is the convolution of $f_{\gamma_{\mathcal{R}_b\mathcal{B}}}(\gamma)$ and $f_{\gamma_{\mathcal{AB}}}(\gamma)$, i.e., $f_{\gamma_B^{\text{coop}}}^{\mathcal{A}\to\mathcal{R}_b\to\mathcal{B}}(\gamma)=f_{\gamma_{\mathcal{R}_b\mathcal{B}}}(\gamma)*f_{\gamma_{\mathcal{AB}}}(\gamma)$. The PDF expression of $\gamma_{\mathcal{R}_b\mathcal{B}}$ can be obtained by

$$f_{\gamma_{\mathcal{R}_b\mathcal{B}}}\left(\gamma\right)=\int_0^\infty\frac{f_{\gamma_{\mathcal{R}_i\mathcal{B}}\mathcal{Z}_i}\left(\gamma,z\right)}{f_{\mathcal{Z}_i}\left(z\right)}f_{\max(\mathcal{Z}_i)}\left(z\right)dz, \tag{55}$$

where $\mathcal{Z}_i=\min(\gamma_{\mathcal{A}\to\mathcal{R}_i},\gamma_{\mathcal{B}\to\mathcal{R}_i})$, and $f_{\mathcal{Z}_i}(z)$ is given in (35). In order to find (55), each part of the integrand has to be calculated separately. The expression for $f_{\mathcal{Z}_i}(z)$ is already given in (35) and the PDF expression of $f_{\gamma_{\mathcal{R}_i\mathcal{B}}\mathcal{Z}_i}(\gamma,z)$ can be obtained from the derivative of joint CDF of $\gamma_{\mathcal{R}_i\mathcal{B}}\mathcal{Z}_i$, which is expressed as

$$F_{\gamma_{\mathcal{R}_i\mathcal{B}},\mathcal{Z}_i}\left(z,\gamma\right)=\Pr[\gamma_{\mathcal{BR}_i}\leq\gamma/\mathcal{K}_{\mathcal{AB}},\mathcal{Z}_i\leq z], \tag{56}$$

TABLE I
SUMMARY OF THE SYMBOLS USED THROUGHOUT THE PAPER

Symbol	Definition	Symbol	Definition
L	Number of relays	$\boldsymbol{r}^{i\to j}$	Node j's signal after reordering received components
h_{ij}	Channel gains	$\overline{P}_{\text{th}}(e)$	Predefined error probability threshold
Ω_{ij}	Variance of channel gains	$\overline{P}_j(e)$	Overall E2E error probability at node j
N_0	Noise variance	$\overline{P}_{\text{coop}}^{i\to\mathcal{R}_k\to j}(e)$	E2E error probability in cooperation case via $\mathcal{R}_k$ node
θ	Rotation angle	$\overline{P}_{\text{direct}}^{i\to j}$	E2E error probability indirect link between i and j nodes
γ_{ij}	SNR between i and j	$\overline{P}_{\text{off},R_k}$	Probability that R_k node cannot decode messages sent by end-sources
β	Normalization parameter	P_T	Total power consumption available in the system
χ	Rotated constellation	$P_i^{\max}$	Total power consumption available at node i
$\boldsymbol{s}$	A pair of signal points from χ	$\mathrm{Q}(\cdot,\cdot;\cdot)$	CCDF of a bivariate Gaussian variable
Λ	Expanded constellation	$\mathcal{K}_{ij}$	Ratio of the transmit powers of relay and the node j for $i\to R_b\to j$ link
λ_i	The i-th symbol from Λ	$F_\gamma(\gamma)$	CDF of γ
P_i	Transmit power at node i	$f_\gamma(\gamma)$	PDF of γ
$y^{i\to j}$	Received signal at node j	$\Im\{.\}$	Quadrature component of a signal point
$\overline{\gamma}_{ij}$	Average SNR between i and j	$\Re\{.\}$	In-phase component of a signal point
D_i	Decision region of i-th symbol	$u(\cdot)$	Unit step function
T_i	Lines bounding D_i	$\delta(\cdot)$	Dirac delta function
C	Decoding set	$\Pr[\cdot]$	Probability

and the derivative of (56), $f_{\gamma_{\mathcal{R}_i\mathcal{B}}Z_i}(\gamma,z)$, can be found as

$$f_{\gamma_{\mathcal{R}_i\mathcal{B}}Z_i}(\gamma,z) = f_{\gamma_{\mathcal{B}\mathcal{R}_i}}\left(\frac{\gamma}{\mathcal{K}_{\mathcal{AB}}}\right) f_{\gamma_{\mathcal{A}\mathcal{R}_i}}(z)\, u\left(\frac{\gamma}{\mathcal{K}_{\mathcal{AB}}}-z\right) + f_{\gamma_{\mathcal{B}\mathcal{R}_i}}\left(\frac{\gamma}{\mathcal{K}_{\mathcal{AB}}}\right)\left(1-F_{\gamma_{\mathcal{A}\mathcal{R}_i}}(z)\right)\delta\left(\frac{\gamma}{\mathcal{K}_{\mathcal{AB}}}-z\right). \tag{57}$$

For the calculation of $f_{\max(\mathcal{Z}_i)}(z)$, which refers to the PDF of $\mathcal{Z}_i$ is the maximum, the CDF expression, $F_{\max(\mathcal{Z}_i)}(z)$, is given by

$$F_{\max(\mathcal{Z}_i)}(z) = \prod_{i=1}^{L}\Pr[\mathcal{Z}_i<z] = \prod_{i=1}^{L}\left(1-e^{-z/\overline{\mathcal{Z}}_i}\right). \tag{58}$$

The derivative of (58) with respect to $\mathcal{Z}_i$ yields to $f_{\max(\mathcal{Z}_i)}(z)$, and $f_{\gamma_{\mathcal{R}_b\mathcal{B}}}(\gamma)$ can be obtained. Under the case of the same average SNRs between the end-sources and the relays, $\overline{\gamma}_{i\mathcal{R}_l}=\overline{\gamma}_{i\mathcal{R}_b}$ and $\overline{\gamma}_{\mathcal{R}_l j}=\overline{\gamma}_{\mathcal{R}_b j}$, $f_{\max(\mathcal{Z}_i)}(z)$ can be obtained as

$$f_{\max(\mathcal{Z}_i)}(z) = \sum_{i=1}^{L}\binom{L}{i}(-1)^{i-1}\frac{i}{\overline{\gamma}}\exp\left(-iz/\overline{\gamma}\right). \tag{59}$$

Substituting (57), (59), and (35) into (55) and taking convolution with $f_{\text{direct}}^{\mathcal{A}\to\mathcal{B}}(\gamma_{\mathcal{B}})$, $f_{\gamma_{\mathcal{B}}^{\text{coop}}}(\gamma)$ can be found as

$$\begin{aligned} f_{\gamma_{\mathcal{B}}^{\text{coop}}}(\gamma) &= \\ \sum_{i=1}^{L}\Bigg\{ &-\mathcal{K}_{\mathcal{AB}}\frac{i(-1)^{(i)}\overline{\gamma}_{\mathcal{B}\mathcal{R}_i}\left(\exp\left(\frac{-\gamma}{\overline{\gamma}_{\mathcal{AB}}}\right)-\exp\left(\frac{-\gamma}{\mathcal{K}_{\mathcal{AB}}\overline{\gamma}_{\mathcal{B}\mathcal{R}_i}}\right)\right)}{\left((i-1)\overline{\gamma}_{\mathcal{A}\mathcal{R}_i}+i\overline{\gamma}_{\mathcal{B}\mathcal{R}_i}\right)\left(\overline{\gamma}_{\mathcal{AB}}-\mathcal{K}_{\mathcal{AB}}\overline{\gamma}_{\mathcal{B}\mathcal{R}_i}\right)} \\ &-\frac{i(-1)^{(i)}\exp\left(\frac{-\gamma}{\overline{\gamma}_{\mathcal{AB}}}\right)\overline{\gamma}_{\mathcal{A}\mathcal{R}_i}\overline{\gamma}_{\mathcal{B}\mathcal{R}_i}}{\left((i-1)\overline{\gamma}_{\mathcal{A}\mathcal{R}_i}+i\overline{\gamma}_{\mathcal{B}\mathcal{R}_i}\right)} \\ &\times\frac{\left(\exp\left(\frac{\gamma}{\overline{\gamma}_{\mathcal{AB}}}-\frac{i\gamma}{\overline{\gamma}\mathcal{K}_{\mathcal{AB}}}\right)\right)}{\left(-\mathcal{K}_{\mathcal{AB}}\overline{\gamma}_{\mathcal{A}\mathcal{R}_i}\overline{\gamma}_{\mathcal{B}\mathcal{R}_i}+i\overline{\gamma}_{\mathcal{AB}}\left(\overline{\gamma}_{\mathcal{A}\mathcal{R}_i}+\overline{\gamma}_{\mathcal{B}\mathcal{R}_i}\right)\right)}\Bigg\} \\ &+\sum_{i=1}^{L}\mathcal{K}_{\mathcal{AB}}\frac{i(-1)^{(i)}\exp\left(\frac{-\gamma}{\overline{\gamma}_{\mathcal{AB}}}\right)\left(\exp\left(\frac{\gamma}{\overline{\gamma}_{\mathcal{AB}}}-\frac{i\gamma}{\overline{\gamma}\mathcal{K}_{\mathcal{AB}}}\right)\right)\overline{\gamma}_{\mathcal{A}\mathcal{R}_i}}{\left(-\mathcal{K}_{\mathcal{AB}}\overline{\gamma}_{\mathcal{A}\mathcal{R}_i}\overline{\gamma}_{\mathcal{B}\mathcal{R}_i}+i\overline{\gamma}_{\mathcal{AB}}\left(\overline{\gamma}_{\mathcal{A}\mathcal{R}_i}+\overline{\gamma}_{\mathcal{B}\mathcal{R}_i}\right)\right)}, \end{aligned} \tag{60}$$

with $\overline{\gamma}=\frac{\overline{\gamma}_{\mathcal{A}\mathcal{R}_i}\overline{\gamma}_{\mathcal{B}\mathcal{R}_i}}{\overline{\gamma}_{\mathcal{A}\mathcal{R}_i}+\overline{\gamma}_{\mathcal{B}\mathcal{R}_i}}$. The resulting error probability for cooperative case $\overline{P}_{\text{coop}}^{\mathcal{A}\to\mathcal{R}_b\to\mathcal{B}}(e)$ can be derived as

$$\overline{P}_{\text{coop}}^{\mathcal{A}\to\mathcal{R}_b\to\mathcal{B}}(e) \approx \sum_{k=0}^{M-1}\sum_{\substack{l=0\\ l\neq k}}^{M-1}\sum_{t=1}^{T_l}\pm\left[B(v_1,\alpha_1)+B(v_2,\alpha_2)\right], \tag{61}$$

where $\alpha_1=\sqrt{2}\mathcal{L}_{l,p_t}(\sqrt{\beta}\chi(k))$, $\alpha_2=\sqrt{2}\mathcal{L}_{l,p_t+1}(\sqrt{\beta}\chi(k))$, $v_1=\upsilon(\alpha_1,\alpha_2,\rho)$, $v_2=\upsilon(\alpha_2,\alpha_1,\rho)$, and $B(v_k,\alpha_k)$ is an auxiliary function as given in (62) at the bottom of the next page.

For convenience, we summarize the symbols used in this paper in Table I.

IV. OPTIMIZATION PROBLEMS: FORMULATION AND ANALYSIS

A. Single Optimization of Rotation Angle

The performance of the proposed SSD-based TDBC protocol heavily depends on the choice of the rotation angle. This is due to the fact that the choice of the rotation angle affects the shape of the expanded constellation Λ, i.e., distance between the constellation symbols in the expanded constellation. It is obvious that a well-chosen rotation angle can lead to a significant gain in the system performance. To that end, assuming that all nodes transmit with the same power, we perform optimization of the rotation angle, θ, in order to minimize the E2E error probability of one of the end-source, while keeping the E2E error probability of the other end-source below a predefined threshold. Then, the rotation angle optimization problem can be formulated as

$$\min_{\theta} \quad \overline{P}_{\mathcal{B}}(e) \tag{63a}$$

$$\text{subject to} \quad \overline{P}_{\mathcal{A}}(e) \leq \overline{P}_{\text{th}}(e), \tag{63b}$$

$$\theta \in (0^\circ,\ 45^\circ), \tag{63c}$$

where θ changes in the range of 0° to 45°.[6]

The given formulation in (63) is a nonconvex program. Since finding an analytical solution to this optimization problem is intractable , we resort to numerical optimization. To obtain the optimal rotation angle, we have used MATLAB optimization toolbox command *fmincon* with interior-point method, which is designed to find the minimum of a given constrained nonlinear multivariable function.

[6]Since the considered constellation is symmetric with respect to the real and the imaginary axes, all possible results can be obtained as θ varies in the range from 0° to 45°. This range is valid for other symmetric constellations, such as QPSK, 8-PSK, 16-QAM, 64-QAM, and so on.

B. Joint Optimization of Rotation Angle and Transmit Power Allocation

In addition to rotation angle θ another important factor affecting the performance of the system is the transmit power employed at end-sources and relays, $P_{\mathcal{A}}$, $P_{\mathcal{B}}$, and $P_{\mathcal{R}}$. To further improve the performance, we consider the rotation angle along with transmit power allocation [23], [24]. In order to simplify the analysis, the optimization of the rotation angle and the transmit power allocation can be considered sequentially. However, such consideration may lead to an inferior system performance. To provide a significant boost in the system performance, we treat the rotation angle and the transmit power allocation jointly.

Similar to the previous section, the design objective is to minimize the E2E error probability of one of the end-sources. To provide a certain level of transmission reliability for the end-source $\mathcal{A}$, the E2E error probability at the end-source $\mathcal{A}$ is constrained by a predetermined threshold, $\overline{P}_{\text{th}}(e)$. We assume that the end-sources and the relays have their own power constraints owing to the individual power supplies, i.e., $P_i \leq P_i^{\max}, i \in \{\mathcal{A}, \mathcal{B}, \mathcal{R}\}$. Additionally, since the effect of interference is not considered in the system, to make the scenarios more practical, the

$$\begin{aligned}
&B\left(v_k, \alpha_k, i\right) = \sum_{i=1}^{L} \binom{L}{i} \Bigg\{ -\overline{\gamma}_{\mathcal{BR}_i}(-1)^i i \mathcal{K}_{\mathcal{AB}} \Bigg(\alpha_k \left(\overline{\gamma}_{\mathcal{BR}_i}\mathcal{K}_{\mathcal{AB}}\right)^{3/2} \arctan\left[\tan(v_k)\sqrt{{\alpha_k}^2 + 2/\left(\overline{\gamma}_{\mathcal{BR}_i}\mathcal{K}_{\mathcal{AB}}\right)}/\alpha_k\right] \\
&\times\left({\alpha_k}^2\overline{\gamma}_{\mathcal{BR}_i}\mathcal{K}_{\mathcal{AB}} + 2\right)^{-1/2} - \alpha_k {\overline{\gamma}_{\mathcal{AB}}}^{3/2} \arctan\left[\sqrt{{\alpha_k}^2 + 2/\overline{\gamma}_{\mathcal{AB}}}\tan(v_k)/\alpha_k\right]/\sqrt{{\alpha_k}^2\overline{\gamma}_{\mathcal{AB}} + 2} + v_k\left(\overline{\gamma}_{\mathcal{AB}} - \overline{\gamma}_{\mathcal{BR}_i}\mathcal{K}_{\mathcal{AB}}\right)\Bigg) \\
&\times\left(2\pi\left(\overline{\gamma}_{\mathcal{AR}_i}(i-1) + \overline{\gamma}_{\mathcal{BR}_i} i\right)\left(\overline{\gamma}_{\mathcal{AB}} - \overline{\gamma}_{\mathcal{BR}_i}\mathcal{K}_{\mathcal{AB}}\right)\right)^{-1}\Bigg\} + \Bigg\{\left(\overline{\gamma}_{\mathcal{AB}} i\left(\overline{\gamma}_{\mathcal{AR}_i} + \overline{\gamma}_{\mathcal{BR}_i}\right) - \overline{\gamma}_{\mathcal{AR}_i}\overline{\gamma}_{\mathcal{BR}_i}\mathcal{K}_{\mathcal{AB}}\right)^{-1}\overline{\gamma}_{\mathcal{AR}_i}\overline{\gamma}_{\mathcal{BR}_i}(-1)^i\mathcal{K}_{\mathcal{AB}} \\
&\times\csc^2(v_k)\left({\alpha_k}^2(-\overline{\gamma}_{\mathcal{AB}}) + \cos(2v_k) - 1\right) \times \Bigg(2\pi\sqrt{{\alpha_k}^2\overline{\gamma}_{\mathcal{AB}} + 2}\left(\overline{\gamma}_{\mathcal{AR}_i} + \overline{\gamma}_{\mathcal{BR}_i}\right)\sqrt{{\alpha_k}^2\overline{\gamma}_{\mathcal{AR}_i}\overline{\gamma}_{\mathcal{BR}_i}\mathcal{K}_{\mathcal{AB}} + 2i\left(\overline{\gamma}_{\mathcal{AR}_i} + \overline{\gamma}_{\mathcal{BR}_i}\right)} \\
&\times\left({\alpha_k}^2\overline{\gamma}_{\mathcal{AB}}\csc^2(v_k) + 2\right)\Bigg)^{-1}\Bigg\} \times \Bigg(\sqrt{{\alpha_k}^2\overline{\gamma}_{\mathcal{AR}_i}\overline{\gamma}_{\mathcal{BR}_i}\mathcal{K}_{\mathcal{AB}} + 2i\left(\overline{\gamma}_{\mathcal{AR}_i} + \overline{\gamma}_{\mathcal{BR}_i}\right)}\arctan\left[\sqrt{{\alpha_k}^2 + 2/\overline{\gamma}_{\mathcal{AB}}}\tan(v_k)/\alpha_k\right]\alpha_k i \\
&\times{\overline{\gamma}_{\mathcal{AB}}}^{3/2}\left(\overline{\gamma}_{\mathcal{AR}_i} + \overline{\gamma}_{\mathcal{BR}_i}\right) - \sqrt{{\alpha_k}^2\overline{\gamma}_{\mathcal{AR}_i}\overline{\gamma}_{\mathcal{BR}_i}\mathcal{K}_{\mathcal{AB}} + 2i\left(\overline{\gamma}_{\mathcal{AR}_i} + \overline{\gamma}_{\mathcal{BR}_i}\right)}\, v_k\sqrt{{\alpha_k}^2\overline{\gamma}_{\mathcal{AB}} + 2}\left(\overline{\gamma}_{\mathcal{AB}} i\left(\overline{\gamma}_{\mathcal{AR}_i} + \overline{\gamma}_{\mathcal{BR}_i}\right) - \overline{\gamma}_{\mathcal{AR}_i}\overline{\gamma}_{\mathcal{BR}_i}\mathcal{K}_{\mathcal{AB}}\right) \\
&-\alpha_k\overline{\gamma}_{\mathcal{AR}_i}\overline{\gamma}_{\mathcal{BR}_i}\mathcal{K}_{\mathcal{AB}}\sqrt{\overline{\gamma}_{\mathcal{AR}_i}\overline{\gamma}_{\mathcal{BR}_i}\mathcal{K}_{\mathcal{AB}}\left({\alpha_k}^2\overline{\gamma}_{\mathcal{AB}} + 2\right)}\arctan\left[\tan(v_k)\sqrt{{\alpha_k}^2 + 2i\left(\overline{\gamma}_{\mathcal{AR}_i} + \overline{\gamma}_{\mathcal{BR}_i}\right)/\left(\overline{\gamma}_{\mathcal{AR}_i}\overline{\gamma}_{\mathcal{BR}_i}\mathcal{K}_{\mathcal{AB}}\right)}/\alpha_k\right]\Bigg) \\
&-\Bigg\{\overline{\gamma}_{\mathcal{AR}_i}(-1)^i\mathcal{K}_{\mathcal{AB}}\csc^2(v_k)\left({\alpha_k}^2(-\overline{\gamma}_{\mathcal{AB}}) + \cos(2v_k) - 1\right) \times \Bigg(2\pi\sqrt{{\alpha_k}^2\overline{\gamma}_{\mathcal{AB}} + 2}\left(\overline{\gamma}_{\mathcal{AR}_i} + \overline{\gamma}_{\mathcal{BR}_i}\right)\left({\alpha_k}^2\overline{\gamma}_{\mathcal{AB}}\csc^2(v_k) + 2\right) \\
&\times\sqrt{{\alpha_k}^2\overline{\gamma}_{\mathcal{AR}_i}\overline{\gamma}_{\mathcal{BR}_i}\mathcal{K}_{\mathcal{AB}} + 2i\left(\overline{\gamma}_{\mathcal{AR}_i} + \overline{\gamma}_{\mathcal{BR}_i}\right)}\left(\overline{\gamma}_{\mathcal{AB}} i\left(\overline{\gamma}_{\mathcal{AR}_i} + \overline{\gamma}_{\mathcal{BR}_i}\right) - \overline{\gamma}_{\mathcal{AR}_i}\overline{\gamma}_{\mathcal{BR}_i}\mathcal{K}_{\mathcal{AB}}\right)\Bigg)^{-1}\Bigg\} \times \Bigg\{\alpha_k{\overline{\gamma}_{\mathcal{AB}}}^{3/2} i\left(\overline{\gamma}_{\mathcal{AR}_i} + \overline{\gamma}_{\mathcal{BR}_i}\right) \\
&\times\arctan\left[\sqrt{{\alpha_k}^2 + 2/\overline{\gamma}_{\mathcal{AB}}}\tan(v_k)/\alpha_k\right]\sqrt{{\alpha_k}^2\overline{\gamma}_{\mathcal{AR}_i}\overline{\gamma}_{\mathcal{BR}_i}\mathcal{K}_{\mathcal{AB}} + 2i\left(\overline{\gamma}_{\mathcal{AR}_i} + \overline{\gamma}_{\mathcal{BR}_i}\right)} - \left(\overline{\gamma}_{\mathcal{AB}} i\left(\overline{\gamma}_{\mathcal{AR}_i} + \overline{\gamma}_{\mathcal{BR}_i}\right) - \overline{\gamma}_{\mathcal{AR}_i}\overline{\gamma}_{\mathcal{BR}_i}\mathcal{K}_{\mathcal{AB}}\right) \\
&\times v_k\sqrt{{\alpha_k}^2\overline{\gamma}_{\mathcal{AB}} + 2}\sqrt{{\alpha_k}^2\overline{\gamma}_{\mathcal{AR}_i}\overline{\gamma}_{\mathcal{BR}_i}\mathcal{K}_{\mathcal{AB}} + 2i\left(\overline{\gamma}_{\mathcal{AR}_i} + \overline{\gamma}_{\mathcal{BR}_i}\right)} - \alpha_k\overline{\gamma}_{\mathcal{AR}_i}\overline{\gamma}_{\mathcal{BR}_i}\mathcal{K}_{\mathcal{AB}}\sqrt{\overline{\gamma}_{\mathcal{AR}_i}\overline{\gamma}_{\mathcal{BR}_i}\mathcal{K}_{\mathcal{AB}}\left({\alpha_k}^2\overline{\gamma}_{\mathcal{AB}} + 2\right)} \\
&\times\arctan\left[\tan(v_k)\sqrt{{\alpha_k}^2 + 2i\left(\overline{\gamma}_{\mathcal{AR}_i} + \overline{\gamma}_{\mathcal{BR}_i}\right)/\left(\overline{\gamma}_{\mathcal{AR}_i}\overline{\gamma}_{\mathcal{BR}_i}\mathcal{K}_{\mathcal{AB}}\right)}/\alpha_k\right]\Bigg\}.
\end{aligned} \tag{62}$$

total power consumption over three time slots is constrained as $P_{\mathcal{A}} + P_{\mathcal{B}} + P_{\mathcal{R}} \leq P_T$, where $P_i^{\max} \leq P_T$, $i \in \{\mathcal{A}, \mathcal{B}, \mathcal{R}\}$, and $P_T \leq P_{\mathcal{A}}^{\max} + P_{\mathcal{B}}^{\max} + P_{\mathcal{R}}^{\max}$.

We express the design that jointly optimizes the rotation angle and the transmit powers in the following form:

$$\min_{\theta,\, \beta,\, P_{\mathcal{A}},\, P_{\mathcal{R}},\, P_{\mathcal{B}}} \quad \overline{P}_{\mathcal{B}}(e) \tag{64a}$$

$$\text{subject to} \quad \overline{P}_{\mathcal{A}}(e) \leq \overline{P}_{\text{th}}(e), \tag{64b}$$

$$P_i \leq P_i^{\max}, \qquad i \in \{\mathcal{A}, \mathcal{B}, \mathcal{R}\}, \tag{64c}$$

$$P_{\mathcal{A}} + P_{\mathcal{B}} + P_{\mathcal{R}} \leq P_T, \tag{64d}$$

$$\beta \in (0,\ 1), \tag{64e}$$

$$\theta \in (0^\circ,\ 45^\circ), \tag{64f}$$

where β is an optimization variable, which controls the allocation of power of the chosen relay among two data transmissions in the third time slot. Hence, the power used by the chosen relay to transmit the message to the end-source $\mathcal{B}$ is βP_R, whereas the power used by the chosen relay to transmit the message to the end-source $\mathcal{A}$ is $(1-\beta)P_R$.

From the formulation given in (64), it can be seen that the constraints (64c), (64d), (64e), and (64f) are linear, and the objective function and constraint (64b) are nonlinear and nonconvex. Hence, the formulation given in (64) is also a nonconvex program, and we resort to numerical optimization using MATLAB command *fmincon* with interior-point method for solving this problem.[7]

V. Numerical Results and Discussions

We provide several numerical results to demonstrate the performance of the SSD-based TDBC protocol with the two different relay-selection strategies, i.e., reactive and proactive relay selections. The derived analytical expressions are validated through Monte Carlo simulation results. The simulation results are obtained assuming that the modulation scheme used in the SSD technique is QPSK. Even though the results are only shown for the end-source $\mathcal{B}$, all discussions given hereinafter apply for the end-source $\mathcal{A}$ as well.

A. Single Optimization of Rotation Angle

In this section, for all simulations, the individual power constraints are assumed to be given by $P_i^{\max} = 0.8P_T$, where $i \in \{\mathcal{A}, \mathcal{B}, \mathcal{R}\}$. We assume that the total power is equally distributed over the end-sources and the chosen relay, and also, the transmit power of the chosen relay is equally allocated among two data transmissions in the third time slot, i.e., equal power allocation (EPA) with $P_{\mathcal{A}} = P_{\mathcal{B}} = P_{\mathcal{R}} = P_T/3$ and $\beta = 0.5$.

1) Reactive Relay-Selection Case: Fig. 3 shows the E2E error probability performance for $L = 2$, considering different rotation angles. It can be observed that the analytical results are in good agreement with the simulation results, and the performance of the system is significantly affected by the value of the rotation angle. In Table II, we present the optimum values of θ_{opt} in degree for various values of P_T/N_0, which we use in order to generate the proposed TDBC (P-TDBC) curve with θ_{opt}.

In Fig. 4, we focus on the impact of the rotation angle on the system performance. To that end, the E2E error probability is plotted versus the rotation angle at the given different SNR values. It is important to note that the optimal rotation angle differs in terms of chosen SNR value as the decision boundaries of the extended constellation is affected by the chosen SNR value. In addition, as the SNR increases, the system performance becomes more sensitive to a change in the rotation angle.

[7]The MATLAB *fmincon* function does not guarantee to find the global optimum for a nonconvex nonlinear problem, and it can get caught in local optimum. Since the optimization problems considered in (63) and (64) are not convex, we cannot guarantee that the global minimum is found. In this paper, our goal is to show that additional performance gains are possible considering optimization of rotation angle and transmit power allocation.

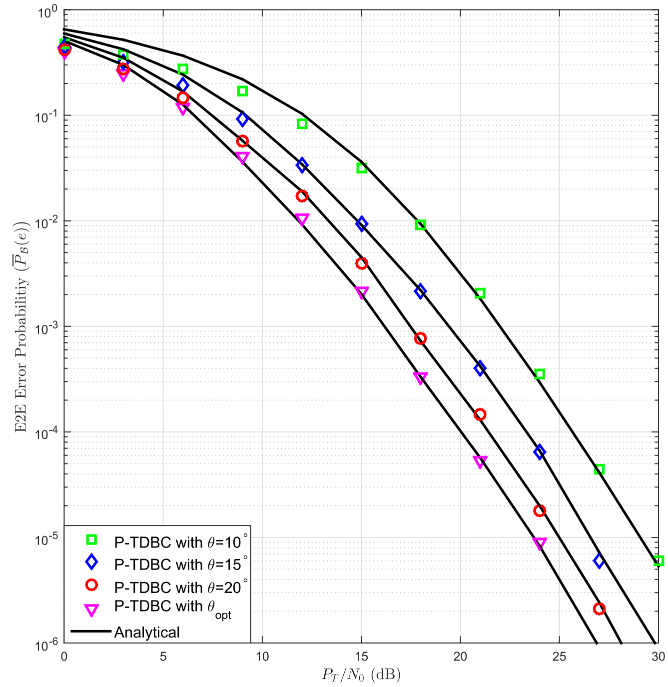

Fig. 3. E2E error probability performance of P-TDBC with the different rotation angles for the reactive relay selection, considering the simulation scenario for $L = 2$ in Table III.

TABLE II
OPTIMUM ROTATION ANGLES FOR REACTIVE RELAY SELECTION ($L = 2, 3$)

$\mathrm{P_T/N_0}$ (dB)	$L = 2$ $\theta_{\text{opt}}(^\circ)$	$L = 3$ $\theta_{\text{opt}}(^\circ)$
0	30.07	29.23
3	28.94	28.50
6	28.31	28.09
9	27.94	27.84
12	27.74	27.69
15	27.63	27.61
18	27.53	27.56
21	27.52	27.54
24	27.52	27.50
27	27.51	27.48
30	27.51	27.43

TABLE III
SIMULATION SCENARIOS

Relay Number	Reactive Relay Selection
$L = 2$	$4\Omega_{\mathcal{AB}} = 1.3\Omega_{\mathcal{BR}_1} = 2\Omega_{\mathcal{AR}_1} = 4\Omega_{\mathcal{BR}_2} = \Omega_{\mathcal{AR}_2}$
$L = 3$	$6\Omega_{\mathcal{AB}} = 2\Omega_{\mathcal{BR}_1} = 3\Omega_{\mathcal{AR}_1} = 6\Omega_{\mathcal{BR}_2} = 1.5\Omega_{\mathcal{AR}_2} = 1.5\Omega_{\mathcal{BR}_3} = \Omega_{\mathcal{AR}_3}$
	Proactive Relay Selection
$L = 2$, and $L = 3$	$4\Omega_{\mathcal{AB}} = 1.3\Omega_{\mathcal{BR}_i} = \Omega_{\mathcal{AR}_i}$, where $i \in \{2, 3\}$.

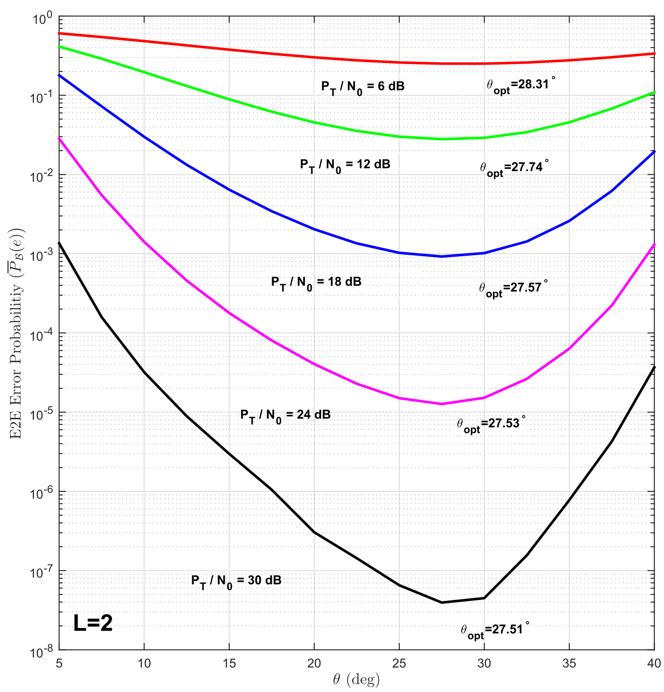

Fig. 4. Effect of choosing different rotation angles θ on the system performance at the different P_T/N_0 values for the reactive relay selection, considering the simulation scenario for $L = 2$ in Table III.

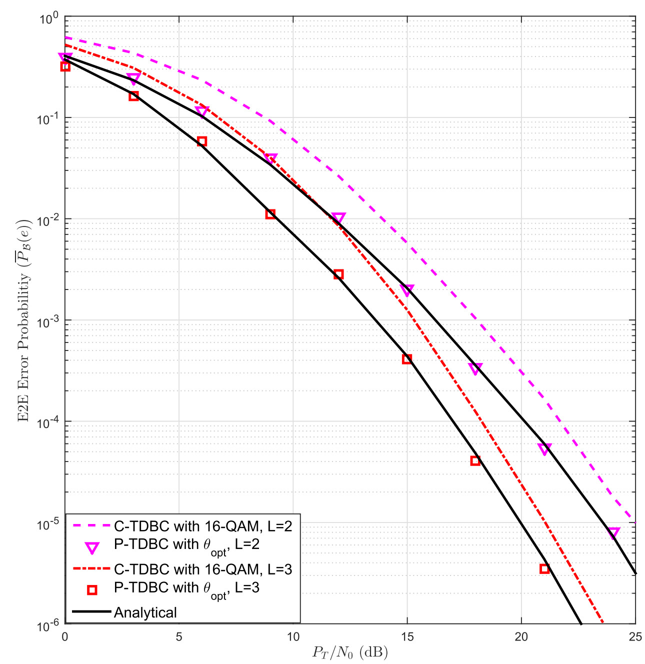

Fig. 5. E2E error probability performance of P-TDBC in compared with C-TDBC for the reactive relay selection, considering the simulation scenarios for $L = 2$ and $L = 3$ in Table III.

Fig. 5 shows the E2E error probability for different number of relays under the assumptions of the optimum rotation angles given in Table II and EPA at the transmitting nodes. It can be seen that the diversity gain increases as the number of relays increases. As a benchmark, in Fig. 5, we provide a comparison against the conventional TDBC two-way relay system, called C-TDBC. For a fair comparison, 16-QAM modulation is considered for C-TDBC to achieve the same spectral efficiency over three time slots. From this figure, it can be seen that the P-TDBC scheme with optimal rotation angles outperforms the C-TDBC over the entire range of SNRs due to achieving both signal space and spatial diversities.

2) Proactive Relay-Selection Case: Similar to the reactive case, in Fig. 6, the E2E error probability for different rotation angles is shown for $L = 3$ case. We can see that the analytical and the simulation results follow the same trend, and the rotation angle influences the system performance. For generating the P-TDBC curve, the optimum values of θ_{opt} in degree for various values of P_T/N_0 are provided in Table IV.

In Fig. 7, we investigate how the system performance is influenced by small changes of the rotation angle at the given SNR

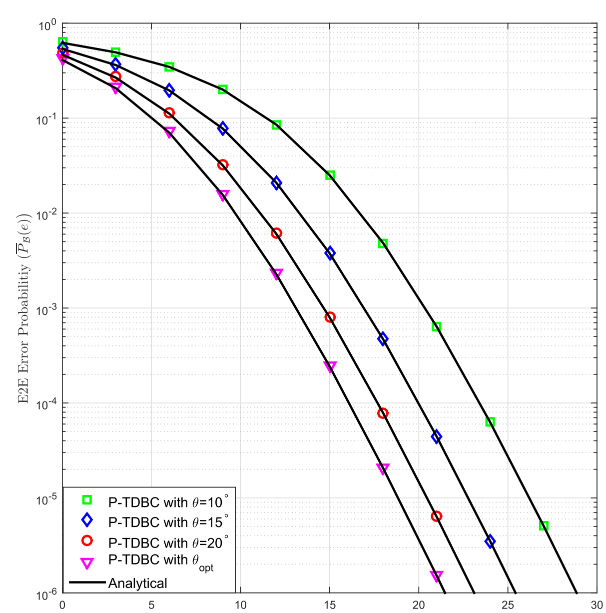

Fig. 6. E2E error probability performance of P-TDBC with the different rotation angles for the proactive relay selection, considering the simulation scenario for $L = 3$ in Table III.

TABLE IV
OPTIMUM ROTATION ANGLES FOR PROACTIVE RELAY SELECTION ($L = 2, 3$)

$\mathrm{P_T/N_0}$ (dB)	$L = 2$ $\theta_{\mathrm{opt}}(^\circ)$	$L = 3$ $\theta_{\mathrm{opt}}(^\circ)$
0	29.16	28.92
3	28.31	28.11
6	27.84	27.67
9	27.58	27.41
12	27.43	27.26
15	27.35	27.17
18	27.30	27.13
21	27.26	27.10
24	27.23	26.91
27	27.19	26.86
30	27.16	26.84

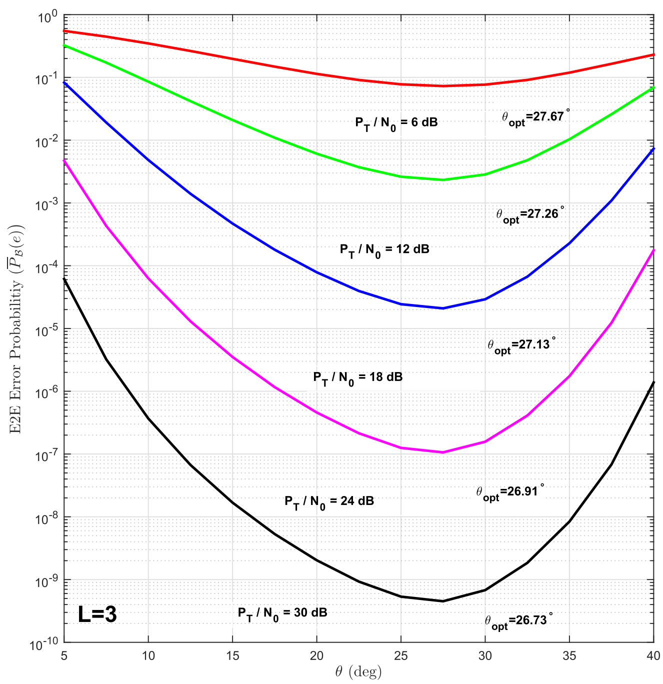

Fig. 7. Effect of choosing different rotation angles θ on the system performance at the different P_T/N_0 values for the proactive relay selection, considering the simulation scenario for $L = 3$ in Table III.

values. It can be observed that the optimal choice of the rotation angle is not the same with all the SNR values. Particularly, in the high SNR values, any deviation from the optimal choice of the rotation angle is more costly in terms of the system performance.

In Fig. 8, we consider a two-way relaying network with different number of relays, assuming the optimum rotation angles given in Table IV and EPA among the transmitting nodes. As expected, when the number of relays increases, the diversity gain increases and the error probability performance enhances. In addition, we give a comparison against the C-TDBC with 16-QAM modulation.

B. Joint Optimization of Rotation Angle and Transmit Power Allocation

1) Reactive Relay-Selection Case: In Fig. 9, the enhancement in the system performance due to the joint optimization of

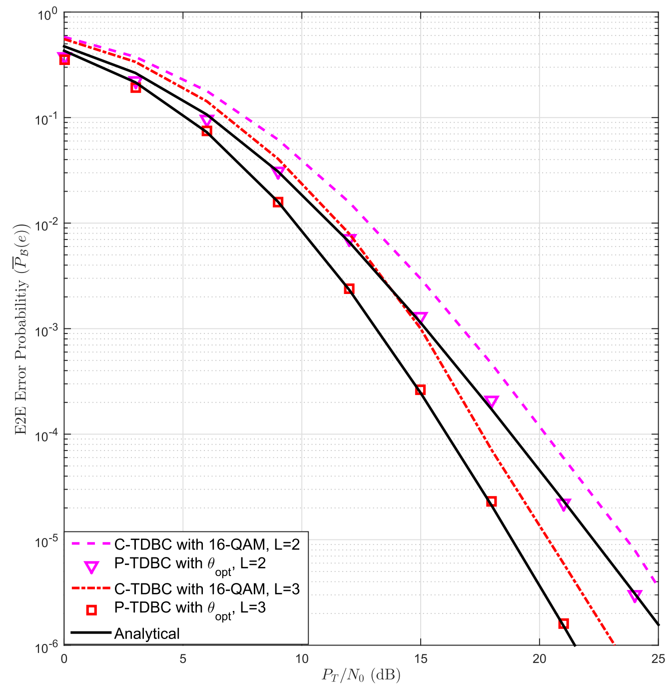

Fig. 8. E2E error probability performance of P-TDBC is compared with C-TDBC for the proactive relay selection, considering the simulation scenarios for $L = 2$ and $L = 3$ in Table III.

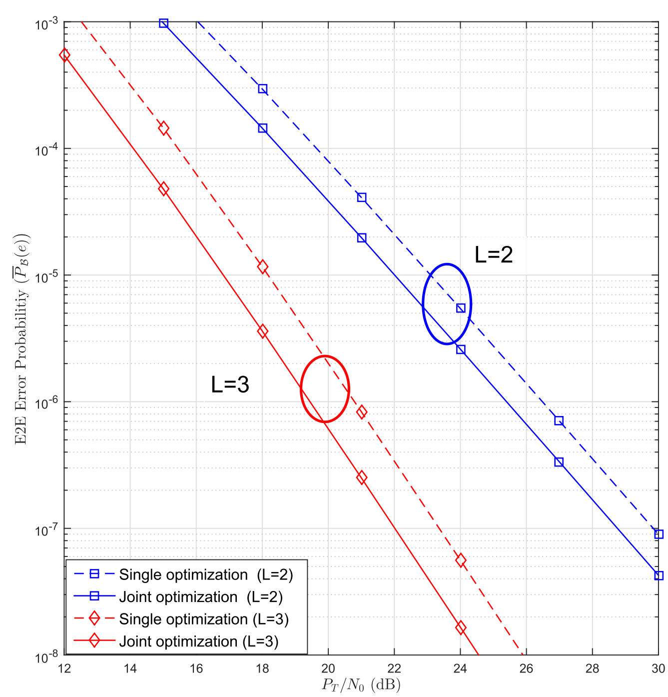

Fig. 9. Effect of the joint optimization of rotation angle and transmit power allocation on the system performance for the reactive relay selection, considering the simulation scenarios for $L = 2$ and $L = 3$ in Table III.

the rotation angle and the transmit power allocation is illustrated for the reactive relay selection. The optimal values of θ_{opt} in degree, $P_{\mathcal{A}}$, $P_{\mathcal{B}}$, $P_{\mathcal{R}}$, and β for various values of P_T/N_0 are shown in Table V. It can be seen that any increase in the SNR value

TABLE V
OPTIMUM ROTATION ANGLES AND POWER ALLOCATION VALUES FOR REACTIVE AND PROACTIVE RELAY SELECTIONS ($L = 2, 3$)

$\mathrm{P_T}/\mathrm{N_0}$ (dB)	Reactive Relay Selection $\{P_{\mathcal{A}}, P_{\mathcal{B}}, P_{\mathcal{R}}, \theta_{\text{opt}}(^\circ), \beta\}$		Proactive Relay Selection $\{P_{\mathcal{A}}, P_{\mathcal{B}}, P_{\mathcal{R}}, \theta_{\text{opt}}(^\circ), \beta\}$	
	$L = 2$	$L = 3$	$L = 2$	$L = 3$
12	{0.302, 0.606, 0.000, 27.67, 0.000}	{0.333, 0.397, 0.269, 27.67, 0.515}	{0.337, 0.572, 0.090, 27.38, 0.090}	{0.414, 0.495, 0.090, 27.21, 0.478}
15	{0.324, 0.480, 0.195, 27.60, 0.452}	{0.422, 0.356, 0.221, 27.59, 0.723}	{0.512, 0.397, 0.090, 27.32, 0.734}	{0.497, 0.412, 0.090, 27.16, 0.749}
18	{0.473, 0.358, 0.171, 27.56, 0.712}	{0.442, 0.368, 0.188, 27.54, 0.814}	{0.522, 0.387, 0.090, 27.29, 0.899}	{0.496, 0.412, 0.090, 27.11, 0.763}
21	{0.498, 0.359, 0.141, 27.53, 0.813}	{0.439, 0.366, 0.177, 27.30, 0.842}	{0.522, 0.387, 0.090, 27.27, 0.897}	{0.478, 0.426, 0.092, 27.10, 0.822}
24	{0.506, 0.368, 0.125, 27.51, 0.876}	{0.367, 0.355, 0.229, 26.64, 0.859}	{0.521, 0.386, 0.091, 27.26, 0.882}	{0.510, 0.386, 0.097, 26.99, 0.891}

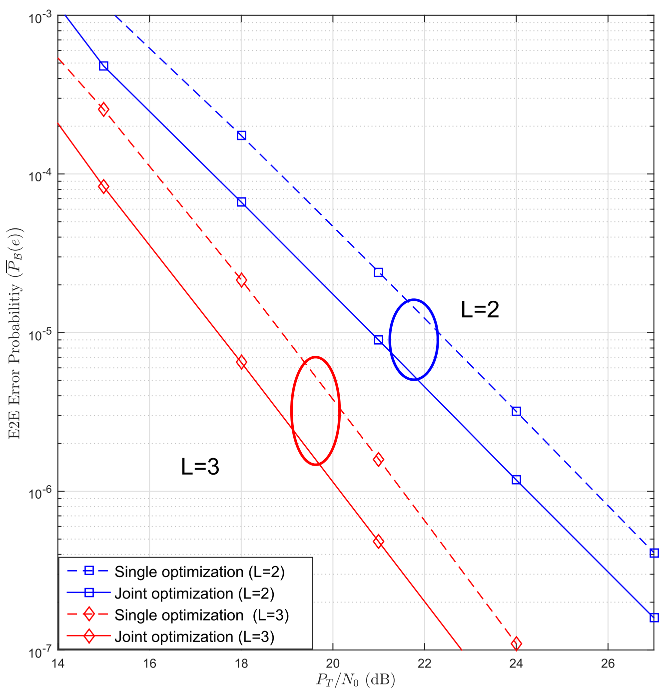

Fig. 10. Effect of the joint optimization of rotation angle and transmit power allocation on the system performance for the proactive relay selection, considering the simulation scenarios for $L = 2$ and $L = 3$ in Table III.

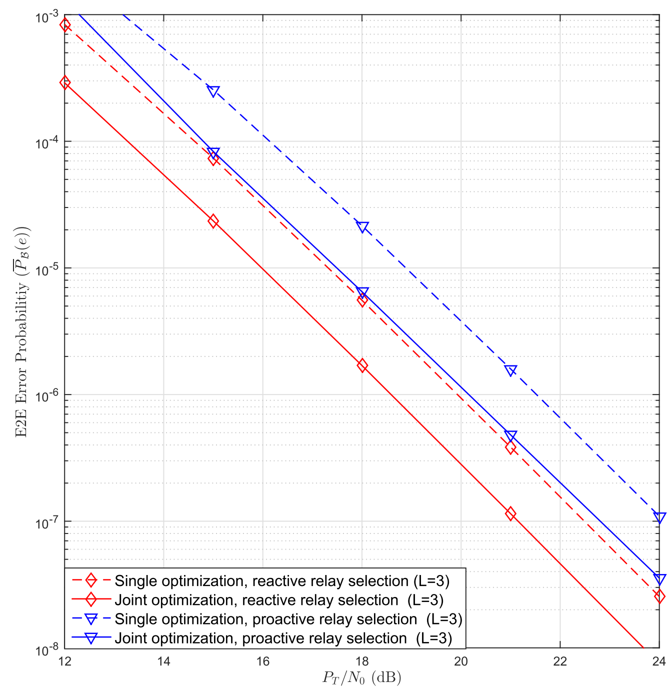

Fig. 11. Comparison of the reactive and proactive relay-selection strategies, considering the simulation scenario for the proactive relay selection with $L = 3$ in Table III.

and in the number of relays affects the system performance in a favorable way.

2) Proactive Relay-Selection Case: In Fig. 10, similar to the reactive relay-selection case, the performance improvement owing to the joint optimization of the rotation angle and the transmit power allocation is depicted. The optimal values of θ_{opt} in degree, $P_{\mathcal{A}}$, $P_{\mathcal{B}}$, $P_{\mathcal{R}}$, and β for various values of P_T/N_0 are provided in Table V. We observe that the transmit power allocation enhances the system performance significantly, and as the number of the relays increases, the system performance improves.

3) Performance Comparison of Reactive and Proactive Relay-Selection Strategies: Finally, in Fig. 11, we compare the performance of the reactive and proactive relay-selection strategies in terms of E2E error probability. Here, we consider the same scenario as the one used for the proactive strategy in the previous section (see Fig. 10) when $L = 3$. Hence, the optimum values provided for the proactive strategy in Table V remain unchanged. However, for that scenario, the optimum values of the reactive strategy can be found in Table VI. From Fig. 11, it can be seen that the reactive strategy shows a superior performance than the proactive one.[8]

TABLE VI
OPTIMUM ROTATION ANGLE AND POWER ALLOCATION VALUES FOR REACTIVE RELAY SELECTION ($L = 3$)

$\mathrm{P_T}/\mathrm{N_0}$ (dB)	$\{P_{\mathcal{A}}, P_{\mathcal{B}}, P_{\mathcal{R}}, \theta_{\text{opt}}(^\circ), \beta\}$
12	{0.367, 0.354, 0.277, 27.64, 0.579}
15	{0.428, 0.353, 0.217, 27.57, 0.736}
18	{0.440, 0.372, 0.184, 27.46, 0.816}
21	{0.411, 0.278, 0.236, 26.64, 0.599}
24	{0.265, 0.278, 0.286, 26.45, 0.592}

[8]Even though the reactive strategy has a superior performance in terms of E2E BER in comparison with the proactive one, it has an inferior performance in terms of energy efficiency [9], [10]. Based on the system designers' preference, either of these strategies can be employed in the system.

VI. Conclusion and Future Works

In this study, an SSD-based TDBC protocol has been considered in multirelay two-way relaying systems to enhance spectral efficiency. The E2E error performance of this protocol has been investigated for the two different relay-selection strategies, i.e., reactive and proactive relay selections. For each relay-selection strategy, we have derived the closed-form expression for the PDF of the output SNR at the end-sources, and obtained the closed-form expression for the E2E error probability, which is valid for any 2-D arbitrary modulation. The obtained E2E error probabilities allow determining the best rotation angle as a function of SNR, and the joint optimization of the rotation angle, and the transmit powers of all nodes. Using the derived expressions, we have first investigated the effect of rotation angle while the transmit power is assumed to be same for all the transmitting nodes. We have observed that the system performance is sensitive to a change in the rotation angle. Then, we have examined the joint effect of the rotation angle and the transmit power on the system performance. We have seen that the optimization of the transmit powers jointly with the rotation angle further improves the system performance. Finally, the numerical results have been revealed that the SSD-based TDBC protocol helps to enhance not only spectral efficiency but also transmission reliability. Other interesting venues for future research would be to include imperfect channel estimation, and to consider a nonreciprocal frequency-selective system.

References

[1] H. U. Sokun, M. C. Ilter, S. Ikki, and H. Yanikomeroglu, "A signal space diversity-based time division broadcast protocol in two-way relay systems," in *Proc. IEEE Global Telecommun. Conf.*, Dec. 2015, pp. 1–6.

[2] Q. Li, R. Q. Hu, Y. Qian, and G. Wu, "Cooperative communications for wireless networks: Techniques and applications in LTE-Advanced systems," *IEEE Wireless Commun.*, vol. 19, no. 2, pp. 22–29, Apr. 2012.

[3] F. Boccardi, R. W. Heath, Jr, A. Lozano, T. L. Marzetta, and P. Popovski, "Five disruptive technology directions for 5G," *IEEE Commun. Mag.*, vol. 52, no. 2, pp. 74–80, Feb. 2014.

[4] W. Chen, "CAO-SIR: Channel aware ordered successive relaying," *IEEE Trans. Wireless Commun.*, vol. 13, no. 12, pp. 6513–6527, Oct. 2014.

[5] A. Sabharwal, P. Schniter, D. Guo, D. W. Bliss, S. Rangarajan, and R. Wichman, "In-band full-duplex wireless: Challenges and opportunities," *IEEE J. Sel. Areas Commun.*, vol. 32, no. 9, pp. 1637–1652, Jun. 2014.

[6] S. Zhang, S. C. Liew, and P. P. Lam, "Hot topic: Physical-layer network coding," in *Proc. ACM Int. Symp. Mobile Ad Hoc Netw. Comput.*, Sep. 2006, pp. 358–365.

[7] S. J. Kim, P. Mitran, C. John, R. Ghanadan, and V. Tarokh, "Coded bi-directional relaying in combat scenarios," in *Proc. IEEE Mil. Commun. Conf.*, Oct. 2007, pp. 1–7.

[8] A. Bletsas, H. Shin, and M. Z. Win, "Cooperative communications with outage-optimal opportunistic relaying," *IEEE Trans. Wireless Commun.*, vol. 6, no. 9, pp. 3450–3460, Sep. 2007.

[9] A. Bletsas, H. Shin, and M. Z. Win, "Outage-optimal cooperative communications with regenerative relays," in *Proc. 40th Annu. Conf. Inf. Sci. Syst.*, Mar. 2006, pp. 632–637.

[10] M. Xia and S. Aïssa, "Fundamental relations between reactive and proactive relay-selection strategies," *IEEE Commun. Lett.*, vol. 19, no. 7, pp. 1249–1252, Jul. 2015.

[11] J. Boutros and E. Viterbo, "Signal space diversity: A power-and bandwidth-efficient diversity technique for the Rayleigh fading channel," *IEEE Trans. Inf. Theory*, vol. 44, no. 4, pp. 1453–1467, Jul. 1998.

[12] S. A. Ahmadzadeh, S. A. Motahari, and A. K. Khandani, "Signal space cooperative communication," *IEEE Trans. Wireless Commun.*, vol. 9, no. 4, pp. 1266–1271, Apr. 2010.

[13] T. Lu, J. Ge, Y. Yang, and Y. Gao, "BEP analysis for DF cooperative systems combined with signal space diversity," *IEEE Commun. Lett.*, vol. 16, no. 4, pp. 486–489, Apr. 2012.

[14] T. Lu, J. Ge, Y. Yang, and Y. Gao, "On bit error performance of full-rate signal space cooperative communication over Nakagami-m fading channels," *IEEE Commun. Lett.*, vol. 16, no. 8, pp. 1224–1227, Aug. 2012.

[15] T. Lu, J. Ge, Y. Yang, and Y. Gao, "Outage probability analysis of signal space cooperative communications over Nakagami-m fading channels," *Electron. Lett.*, vol. 49, no. 18, pp. 1186–1188, Aug. 2013.

[16] R. Mesleh, S. S. Ikki, and O. Amin, "Enhancing cooperative communication spectral efficiency through signal space diversity," in *Proc. IEEE Wireless Commun. Netw. Conf.*, Apr. 2014, pp. 666–670.

[17] O. Amin, R. Mesleh, S. S. Ikki, M. H. Ahmed, and O. A. Dobre, "Performance analysis of multiple-relay cooperative systems with signal space diversity," *IEEE Trans. Veh. Technol.*, vol. 64, no. 8, pp. 3414–3425, Aug. 2015.

[18] L. Szczecinski, H. Xu, X. Gao, and R. Bettancourt, "Efficient evaluation of BER for arbitrary modulation and signaling in fading channels," *IEEE Trans. Commun.*, vol. 55, no. 11, pp. 2061–2064, Nov. 2007.

[19] L. Szczecinski, S. Aissa, C. Gonzalez, and M. Bacic, "Exact evaluation of bit- and symbol-error rates for arbitrary 2-D modulation and nonuniform signaling in AWGN channel," *IEEE Trans. Commun.*, vol. 54, no. 6, pp. 1049–1056, Jun. 2006.

[20] M. K. Simon, "A simpler form of the Craig representation for the two-dimensional joint Gaussian Q-function," *IEEE Commun. Lett.*, vol. 6, no. 2, pp. 49–51, Feb. 2002.

[21] Z. Libo, F. Alajaji, and G. Takahara, "Error analysis for nonuniform signaling over Rayleigh fading channels," *IEEE Trans. Commun.*, vol. 53, no. 1, pp. 39–43, Jan. 2005.

[22] S. M. Ross, *Introduction to Probability Models*. New York, NY, USA: Academic, 2014.

[23] Y. Yang, W. Chen, O. Li, and L. Hanzo, "Variable-rate, variable-power network-coded-QAM/PSK for bi-directional relaying over fading channels," *IEEE Trans. Commun.*, vol. 62, no. 10, pp. 3631–3643, Sep. 2014.

[24] Y. Yang, W. Chen, O. Li, and L. Hanzo, "Joint rate and power adaptation for amplify-and-forward two-way relaying relying on analog network coding," *IEEE Access*, vol. 4, pp. 2465–2478, May 2016.

Hamza Sokun (S'14) received the B.Sc. (Hons.) degree in electronics engineering from Kadir Has University, Istanbul, Turkey, in 2010, and the M.Sc. degree in electrical and electronics engineering from Ozyegin University, Istanbul, Turkey, in 2012. He is currently working toward the Ph.D. degree in electrical and computer engineering from Carleton University, Ottawa, ON, Canada.

His research interests include cooperative communications, green communications, radio resource allocation, and applications of optimization for wireless communications.

Mehmet Cagri Ilter (S'11) received the B.Sc. degree in telecommunication engineering and the M.A.Sc. degree in electronics and communication engineering from Istanbul Technical University, Istanbul, Turkey, in 2009 and 2013, respectively.

He is currently a Research Assistant with Carleton University, Ottawa, ON, Canada, and a member of the 5G research project with Huawei Technologies. His research interests include 5G networks, constellation and encoder design, error correcting codes, network coding, network coded cooperation, signal space diversity, applied probability, and applications of optimization in wireless networks.

Salama Ikki (M'15) received the B.S. degree from Al-Isra University, Amman, Jordan, in 1996, the M.Sc. degree from the Arab Academy for Science and Technology and Maritime Transport, Alexandria, Egypt, in 2002, and the Ph.D. degree from Memorial University, St. Johns, NF, Canada, in 2009, all in electrical engineering.

He is currently an Assistant Professor of wireless communications in the Department of Electrical Engineering, Lakehead University, Thunder Bay, ON, Canada. He was a Research Assistant at the Institut national de la recherche scientifique, University of Quebec, Montreal, QC, Canada, from February 2010 to December 2012 and a Postdoctoral Fellow with the University of Waterloo, Waterloo, ON, Canada, from February 2009 to February 2010. He has been carrying out research in communications and signal processing for more than ten years. During this time, he has authored or coauthored more than 100 papers in the peer-reviewed IEEE international journals and conferences with more than 2500 citations and has a current H-index of 28.

Dr. Ikki received the Best Paper Award published in the *EURASIP Journal on Advanced Signal Processing*. He also received the Exemplary Reviewer Certificate from the IEEE COMMUNICATIONS LETTERS and the IEEE WIRELESS COMMUNICATIONS LETTERS in 2012, and the Top Reviewer Certificate from the IEEE TRANSACTIONS ON VEHICULAR TECHNOLOGY in 2015. His Ph.D. student received the second place for the Best Poster Award at the School of Electrical and Electronic Engineering, Newcastle University, UK Annual Research Conference, January 2014. He currently serves on the editorial boards of the IEEE COMMUNICATIONS LETTERS and the IET Communications Proceeding. He is widely recognized as an expert in the field of wireless communications.

Halim Yanikomeroglu (S'96–M'98–SM'12–F'17) was born in Giresun, Turkey, in 1968. He received the B.Sc. degree in electrical and electronics engineering from the Middle East Technical University, Ankara, Turkey, in 1990, and the M.A.Sc. degree in electrical engineering and the Ph.D. degree in electrical and computer engineering from the University of Toronto, Toronto, ON, Canada, in 1992 and 1998, respectively.

From 1993 to 1994, he was with the Research and Development Group of Marconi Kominikasyon A. S., Ankara, Turkey. Since 1998, he has been with the Department of Systems and Computer Engineering, Carleton University, Ottawa, ON, Canada, where he is currently a Full Professor. From 2011 to 2012, he was a Visiting Professor with the TOBB University of Economics and Technology, Ankara. In recent years, his research has been funded by Huawei, Telus, Allen Vanguard, Blackberry, Samsung, Communications Research Centre of Canada, and DragonWave. This collaborative research resulted in more than 25 patents (granted and applied). His research interests include wireless technologies with a special emphasis on wireless networks.

Dr. Yanikomeroglu received the IEEE Ottawa Section Outstanding Educator Award in 2014, the Carleton University Faculty Graduate Mentoring Award in 2010, the Carleton University Graduate Students Association Excellence Award in Graduate Teaching in 2010, and the Carleton University Research Achievement Award in 2009. He is a Registered Professional Engineer in ON, Canada. He has been involved in the organization of the IEEE Wireless Communications and Networking Conference (WCNC) from its inception, including serving as a Steering Committee Member and the Technical Program Chair or Co-Chair of the WCNC 2004, Atlanta, GA, USA, the WCNC 2008, Las Vegas, NV, USA, and the WCNC 2014, Istanbul, Turkey. He was the General Co-Chair of the IEEE Vehicular Technology Conference (VTC) 2010-Fall held in Ottawa, and he is currently serving as the General Chair of the IEEE VTC 2017-Fall, which will be held in Toronto. He has served on the Editorial Boards of the IEEE TRANSACTIONS ON COMMUNICATIONS, the IEEE TRANSACTIONS ON WIRELESS COMMUNICATIONS, and the IEEE COMMUNICATIONS SURVEYS AND TUTORIALS. He was the Chair of the IEEE Wireless Technical Committee. He is a Distinguished Lecturer of the IEEE Communications Society and a Distinguished Speaker of the IEEE Vehicular Technology Society.